# CHAPTER 4
# RESULTS AND DISCUSSIONS

## 4.1 Dymanic modeling of SOFC

The dynamic modeling of SOFC during the starting-up period (heated by hot nitrogen, hydrogen and syngas) was initially simulated at 500 K and 1 bar. In the case of nitrogen feed, a temperature of 1173K was fed to fuel channel whereas the inlet air was fed to the cathode at the same temperature. It should be noted that SOFC load voltage was kept constant at 0.7 V and the fuel utilization (for the case of hydrogen and syngas feeds) was always kept at 80%. Under heating-up conditions, the characteristics of this SOFC system were predicted in terms of product gas distribution and temperature gradient (with time) along the system.

As the next step, the dynamic modeling of SOFC operated as IIR-SOFC operation and fueled with hydrocarbon compounds (i.e. methane, methanol and ethanol) during heating-up period was studied for comparison. Details of each study are presented as follow:

### 4.1.1 SOFC heating up with nitrogen

Fig. 4.1 (a)-(f) presents the temperature gradiant along the cell at each period. Firstly, the cell was placed in initial condition, in which temperature profile along the cell is shown in Fig. 4.1 (a). After nitrogen hot gas was fed into the cell, the temperature of the cell increases due to the heat transfer from hot gas to the cell as shown in Fig.4.1 (b). Since nitrogen is an inert gas, no reaction occurs at the anode of the cell and the temperature mainly increases by the het reansfer from nitrogen hot gas. Therefore, it takes a long time to increase temperature along the cell to minimum operating temperature. Fig. 4.1 (c)-(f) show temparature profile after initial fed hot gas to cell in 30mins, 2hours, 12 hours, and 30 hours respectively. It can be seen that the temperature of cell reaches 1173 K after 30 hours. Since it takes significantly long time for heat-up, this starting-up pattern is not a suitable option.

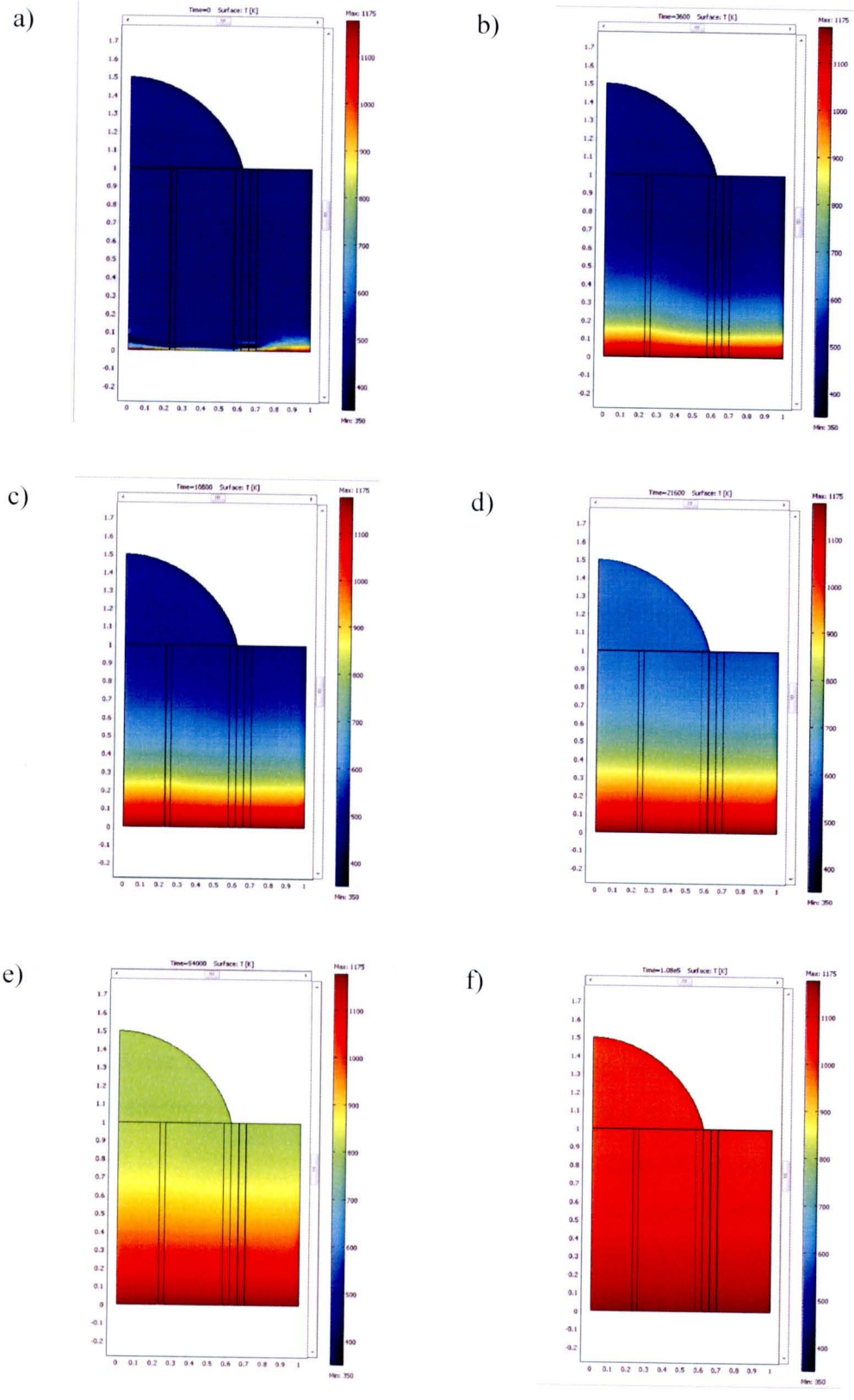


**Figure 4.1** Temperature distribution of heat-up by hot nitrogen gas at (a) 0s, (b) 1 hour, (c) 3 hours, (d) 6 hours, (e) 15 hours, (f) 30 hours.

### 4.1.2 SOFC heating up with hydrogen

For comparison, hydrogen was chosen as the heating gas instead of nitrogen. Fig.4.2 shows the temperature gradients of the cell that fed hydrogen for heating up. It should be noted that hydrogen is a major fuel for SOFC; hence the exothermic electrochemical reaction occurs at the anode of SOFC during the starting-up period. The heat of reaction from the electrochemical reaction consequently results in the reducing of time duration in the heating-up period. It can be seen from Fig. 4.2 that the temperature of the system reaches 1173 K after only 2 minutes and reaches steady state after 1 hour. Although this heat-up pattern provides the shortest starting-up time, the extremely high heating rate (0.93 K/s) could result in the high thermal stress of material and consequently damage the SOFC system. [Barzi *et al.* (2009)]

Fig 4.3 and Fig 4.4 present the concentration gradient of $H_2$ and $H_2O$ generated along the IIR-SOFC system with time from the electrochemical reaction. It can be seen that hydrogen disseminates along IIR-SOFC and changes to steam at the anode of SOFC.

### 4.1.3 SOFC heating up with syngas

In order to reduce the rapid temperature rising during the starting-up period due to the too high electrochemical reaction of hydrogen, syngas (the mixture of CO 50%and $H_2$ 50%) was applied instead. Fig. 4.5 presents the temperature gradient by time of SOFC using syngas for heating-up. It should be noted that syngas consists of $H_2$ and CO, which are also the possible fuel for SOFC; nevertheless, the electrochemical reaction rate of CO is relatively lower than $H_2$, hence the rapid temperature rising up would be reduced. It can be seen from Fig. 4.5 that the temperature of the system also increases due to exothermic electrochemical reaction but with the lower rate than that using $H_2$. In the case of syngas heating-up, SOFC temperature reaches 1173 K after 30 minutes and becomes steady after 2 hours. For the calculation, it was observed that the heating using syngas is 0.37 K/s. With this heating-up rate, it is compatible with SOFC material, from which the heating rate should be around 0.5 K/s.

Figs. 4.6 – 4.10 present the concentration gradients of syngas composition as well as the products from the electrochemical reaction including $H_2$, $H_2O$, CO and $CO_2$ at various times. It can be seen that the profiles of $H_2$ and CO decrease steadily with time, whereas those of $CO_2$ and $H_2O$ increases with increasing operating time.

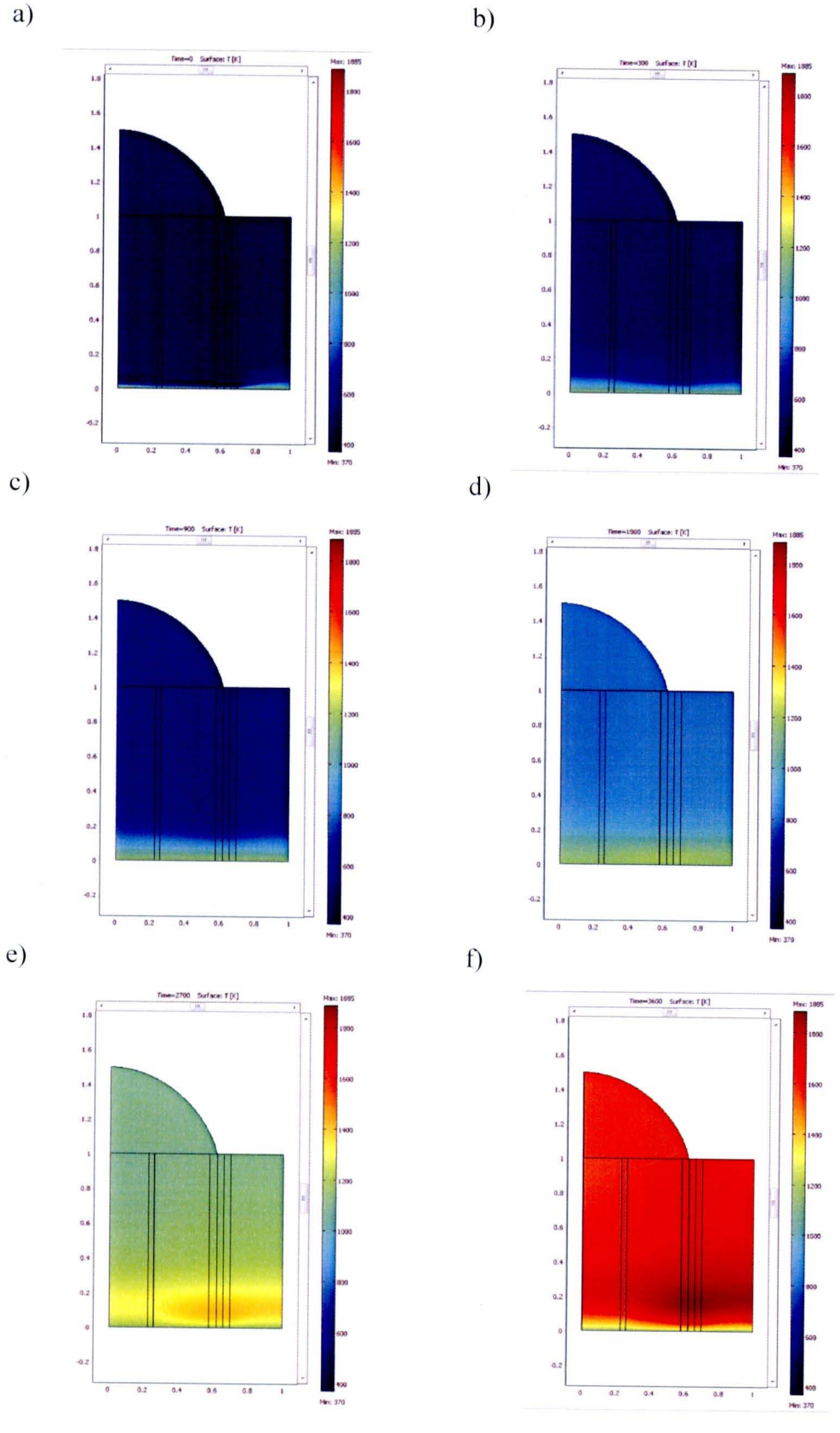


**Figure 4.2** Temperature distribution of heat-up by hydrogen at (a) 0s, (b) 5 mins, (c) 15 mins, (d) 30 mins, (e) 45 mins, (f) 1 hour.

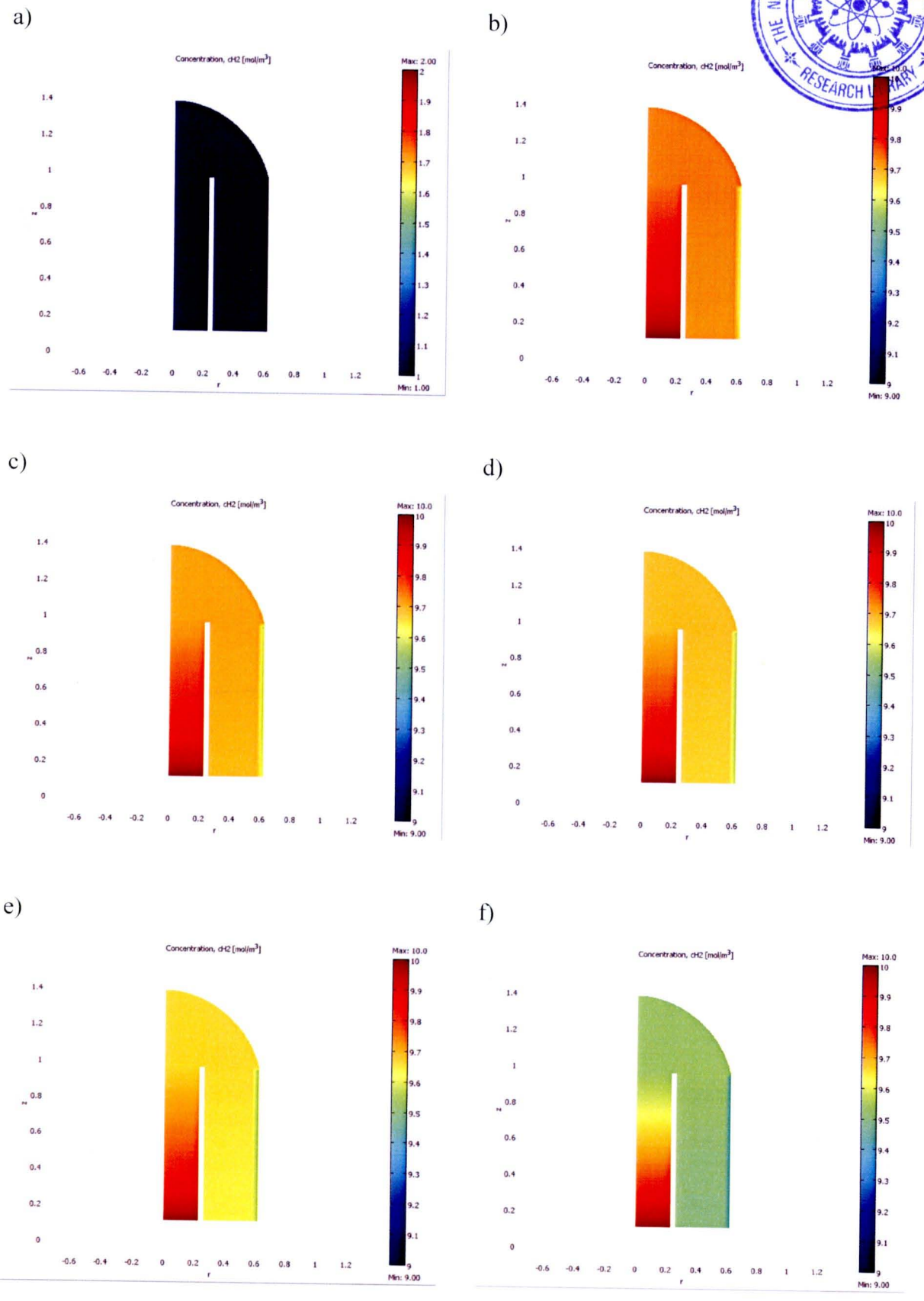


**Figure 4.3** Concentration of $H_2$ along the cell for hydrogen heat up gas at a) 0s, (b) 5 min, (c) 15 mins,(d) 30 mins, (e) 45 mins, (f) 1 hour.

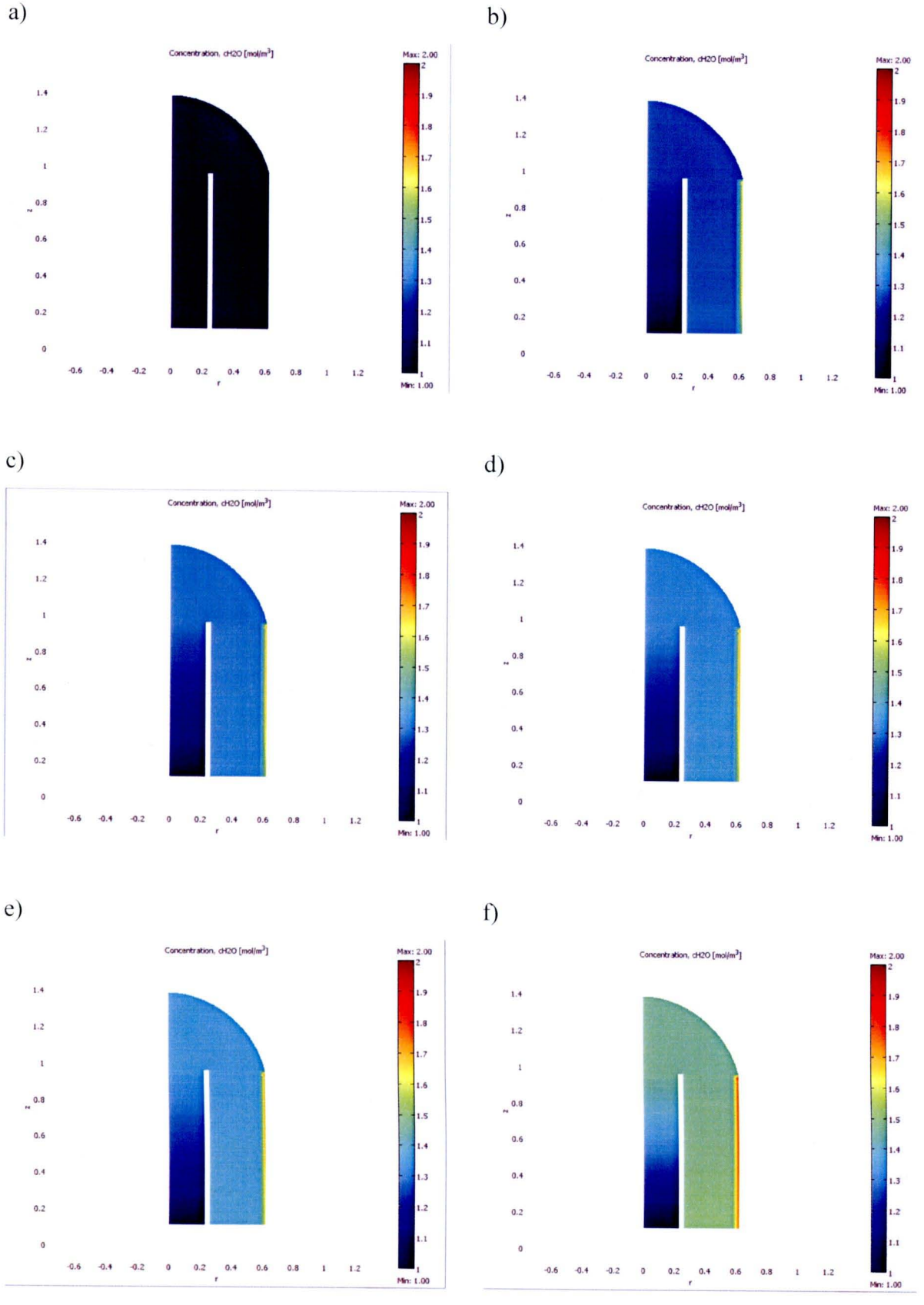


**Figure 4.4** Concentration of $H_2O$ along the cell for hydrogen heat up gas at a) 0s, (b) 5 mins, (c) 15 mins,(d) 30 mins, (e) 45 mins, (f) 1 hour.

a)

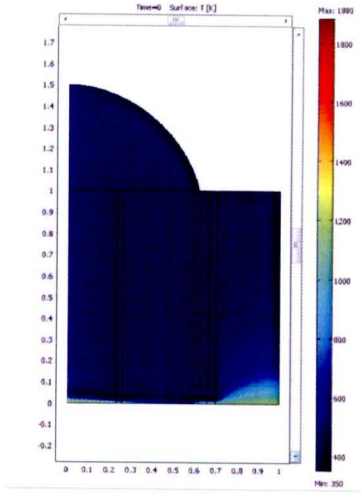

b)

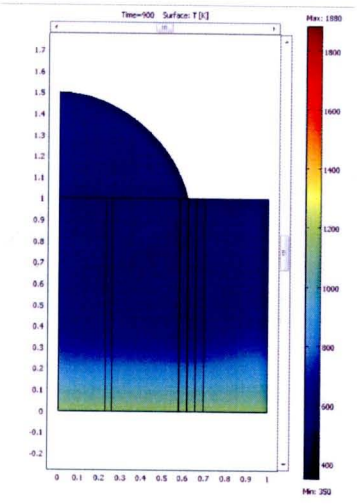

c)

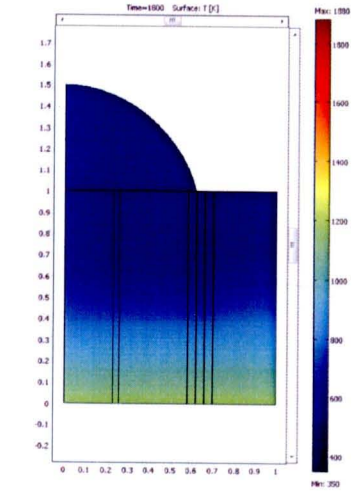

d)

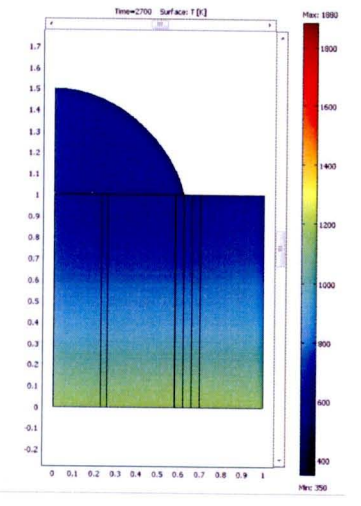

e)

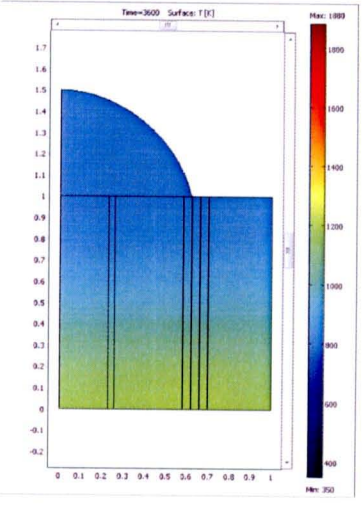

f)

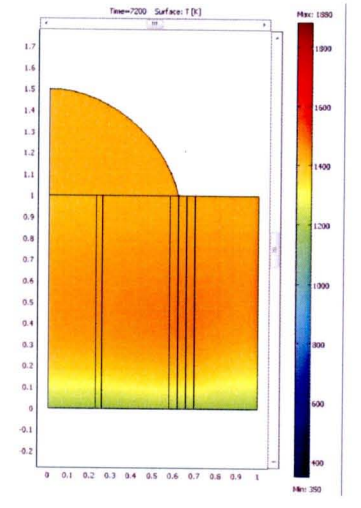

**Figure 4.5** Temperature distribution of heat-up by syngas at (a) 0s, (b) 15 mins, (c) 30 mins, (d) 45 mins, (e)1 hour, (f) 2 hours.

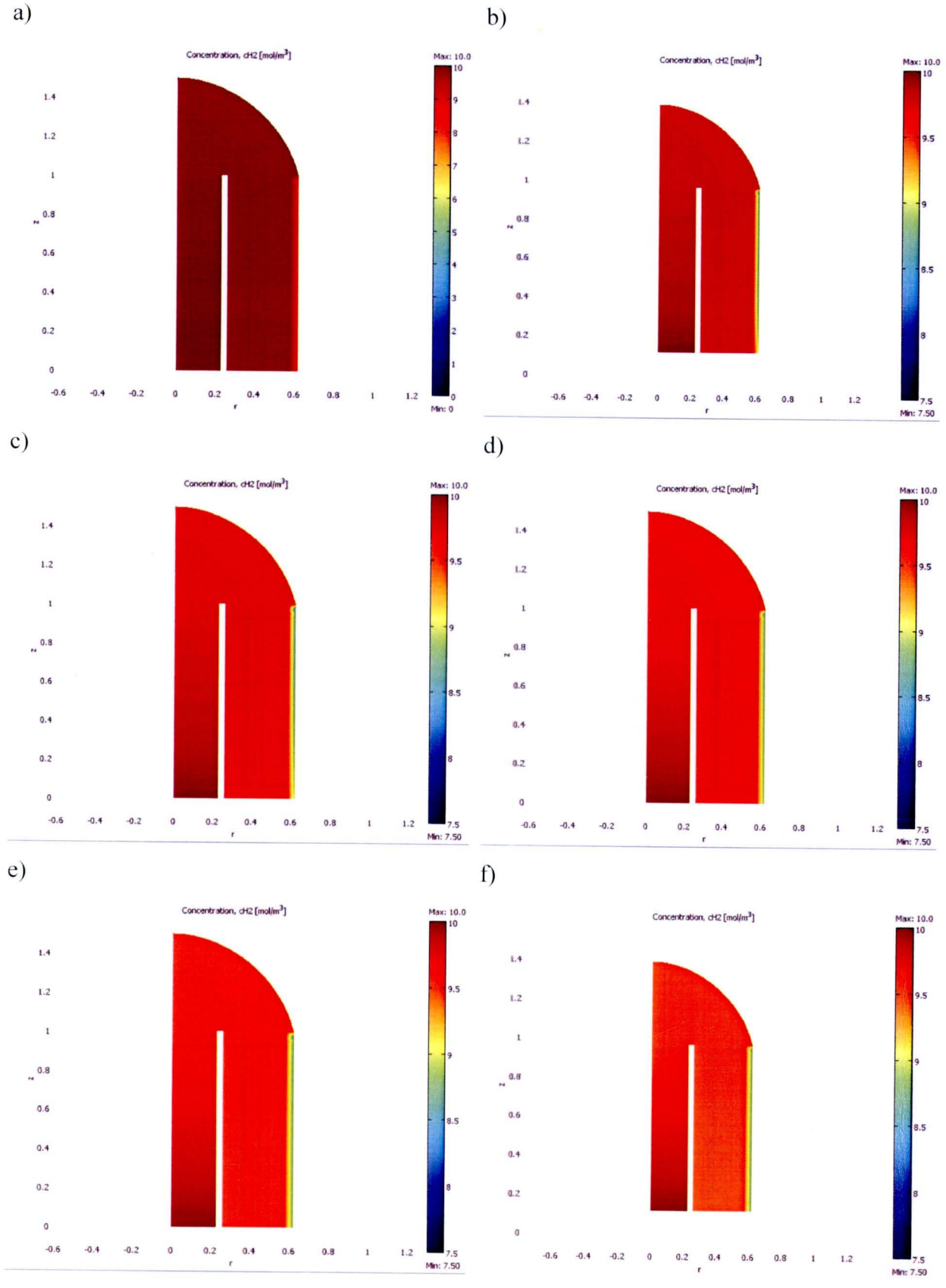


**Figure 4.6** Concentration of $H_2$ along the cell for syngas heat up gas at (a) 0s, (b) 6 mins, (c) 24 mins, (d) 1 hours, (e) 1.5 hours, (f) 2 hours.

a)

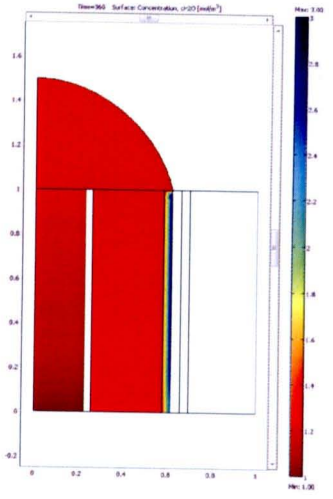

b)

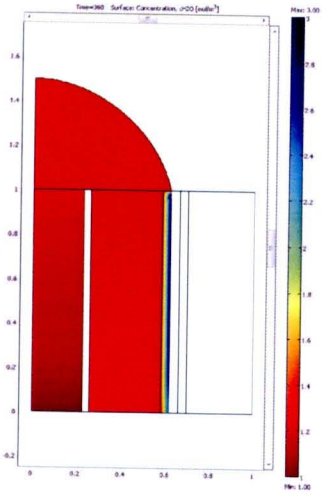

c)

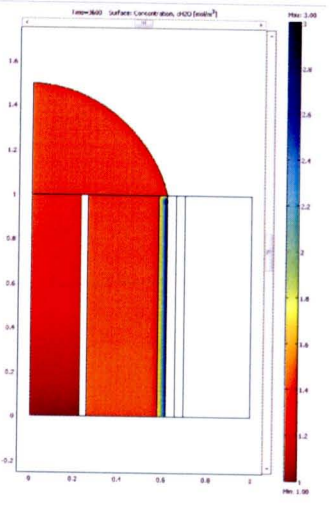

d)

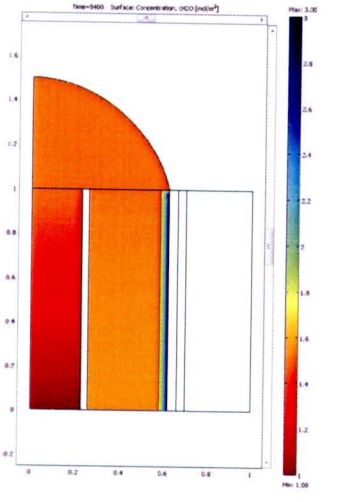

e)

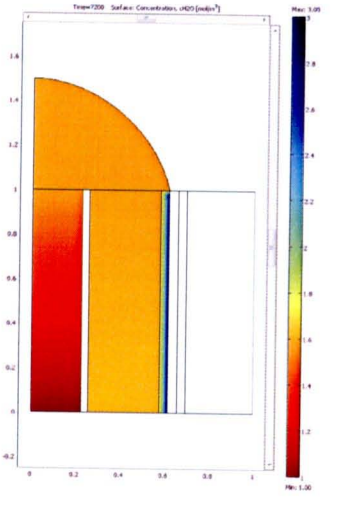

f)

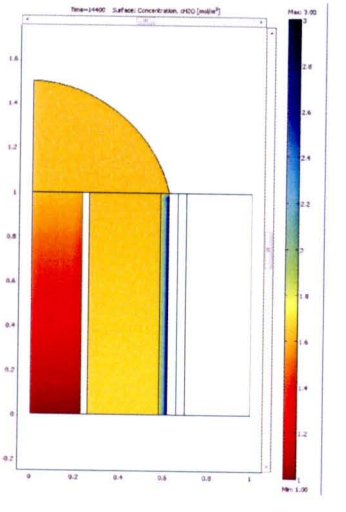

**Figure 4.7** Concentration of $H_2O$ along the cell for syngas heat up gas at (a) 0s, (b) 6 mins, (c) 24 mins, (d) 1 hours, (e) 1.5 hours, (f) 2 hours.

a)

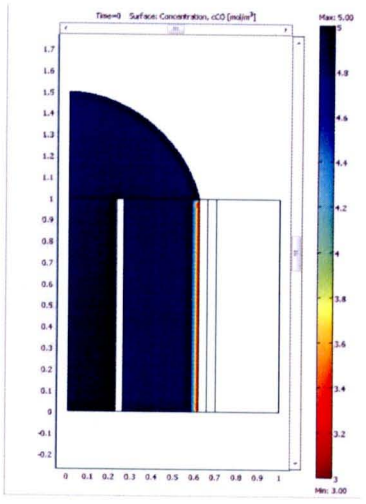

b)

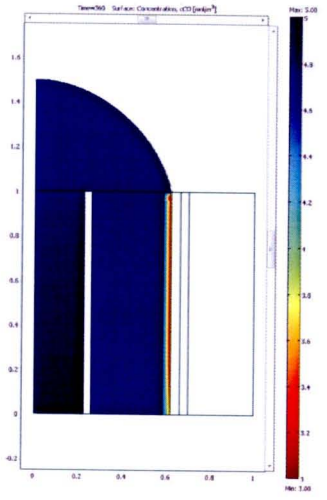

c)

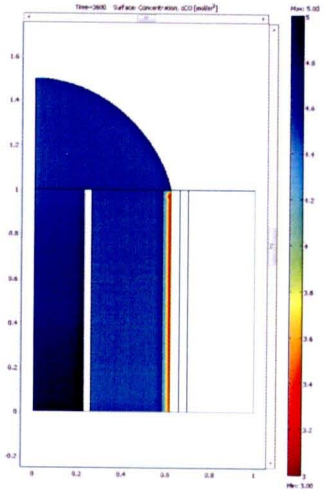

d)

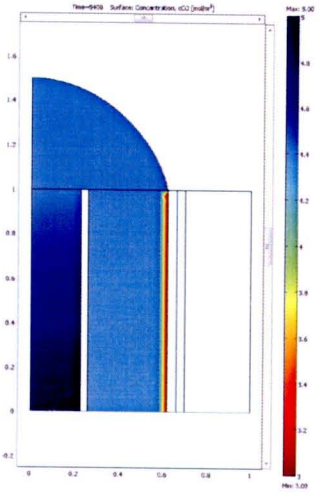

e)

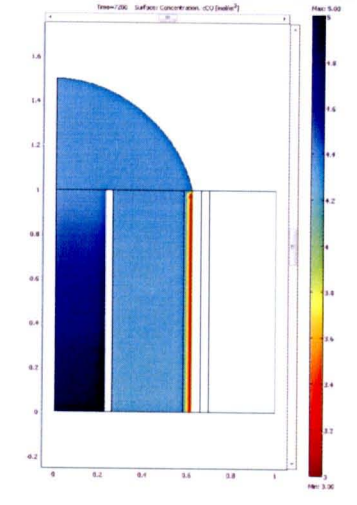

f)

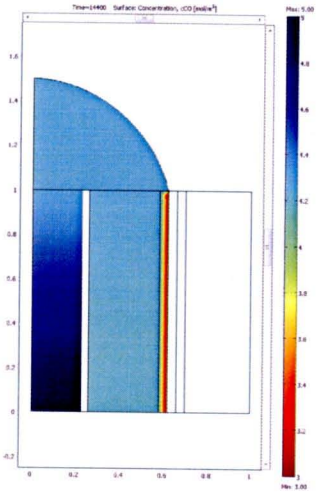

**Figure 4.8** Concentration of CO along the cell for syngas heat up gas at (a) 0s, (b) 6 mins, (c) 24 mins, (d) 1 hours, (e) 1.5 hours, (f) 2 hours.

a)

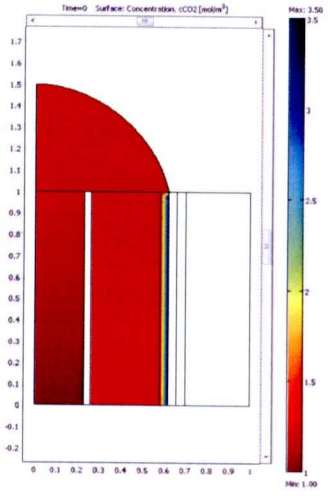

b)

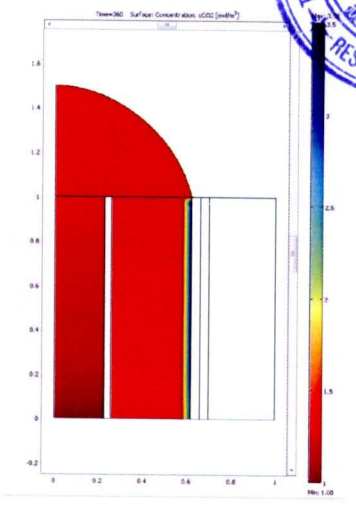

c)

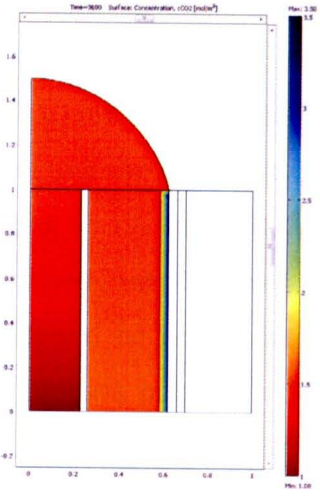

d)

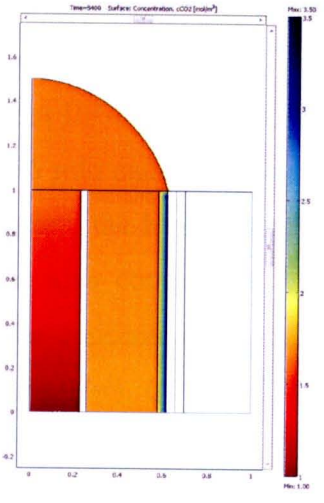

e)

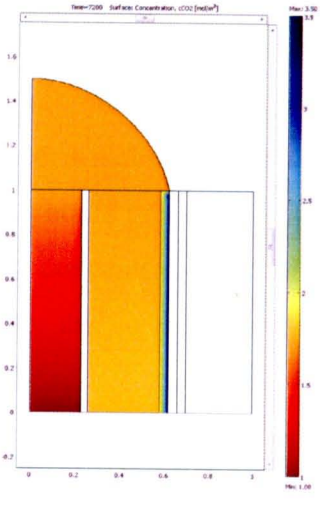

f)

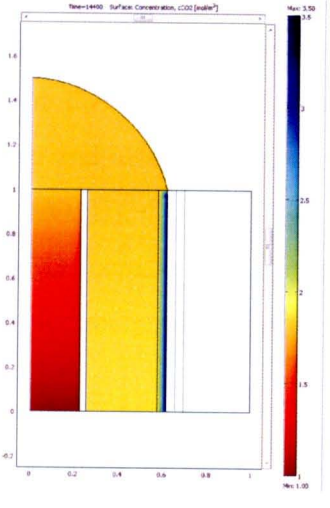

**Figure 4.9** Concentration of $CO_2$ along the cell for syngas heat up gas at (a) 0s, (b) 6 mins, (c) 24 mins, (d) 1 hours, (e) 1.5 hours, (f) 2 hours.

### 4.1.4 IIR-SOFC heating up with methane

As the next step, the direct use of hydrocarbon fuel as primary fuel for SOFC under IIR-SOFC operation was investigated. Firstly, methane was selected as the base case for this study since it is the most common hydrocarbon fuel for SOFC. In this study, the IIR-SOFC operation was simulated by applying internal coated-wall reformer configuration at the inner side of the tubular SOFC since we have previously reported that this IIR-SOFC configuration can enhance high efficiency with low pressure drop problem.

In detail, methane was fed along with steam (S/C ratio= 3:1) to the internal reformer section and reformed to syngas ($H_2$ and CO); it should be noted that the endothermic steam reforming reaction takes place at this section. Then, syngas generated from this reformer was passed continuously through the fuel channel, where the exothermic electrochemical reaction occurs. Under this operation, the heat generated from exothermic electrochemical reaction at the anode side of SOFC can transfer though the internal reforming part.

Fig. 4.10 presents the temperature gradient with time of IIR-SOFC fueled by methane. It can be seen that the temperature can reach 1173 K after 36 min and continuously increase before reaching steady state after 2 hours. Under this operation, the heating rate during this starting-up period was observed to be 0.31 K/s, which is also compatible with the cell material. It should be noted that Figs. 4.11-4.15 present the concentration gradients of all gaseous composition present in the system including $CH_4$, $H_2$, $H_2O$, CO and $CO_2$. It can be seen that the concentration of methane initially rises up in all sections of SOFC (including the reformer and fuel channels). Nevertheless, after 1 hour, the methane profile starts to drop down, particularly in the fuel channel. After 2 hours, the concentration of methane in the fuel channel is close to 0; whereas it decreases along the internal reformer and becomes 0 at the end of the reformer. This could be due to the increase of the system temperature with operating time, which increases the rates of steam reforming and electrochemical reactions; hence, after 2 hours methane in the system are converted to CO, $H_2$, $CO_2$ and $H_2O$. It can be seen that the concentration profiles of CO, $H_2$, $CO_2$ and $H_2O$ increase with increasing the operating time due to the increase of steam reforming and electrochemical reaction rates as mentioned above.

a)

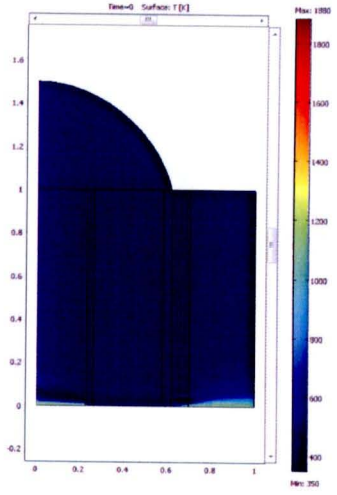

b)

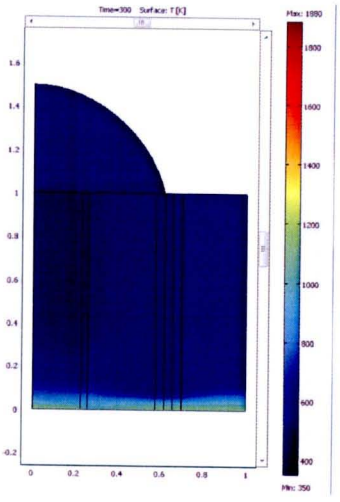

c)

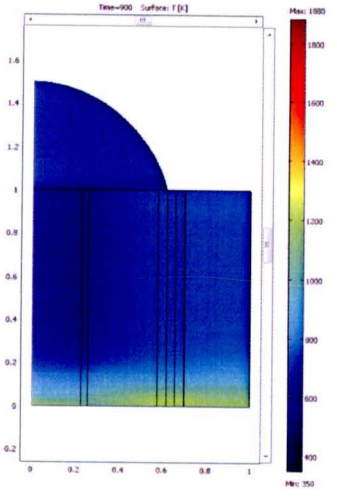

d)

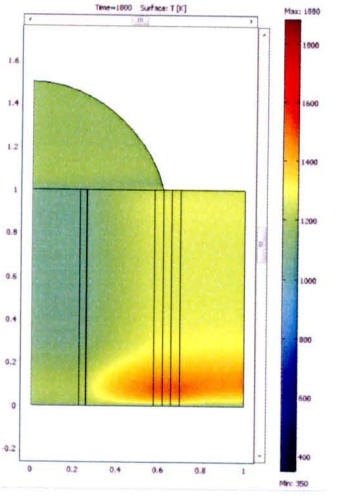

e)

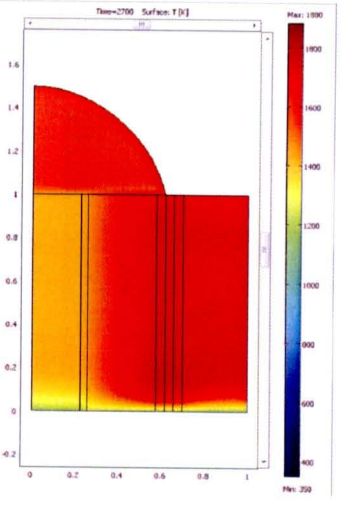

f)

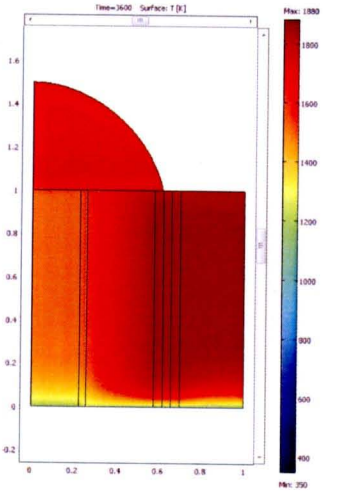

**Figure 4.10** Temperature distribution of heat-up by methane at (a) 0s, (b) 5 mins, (c) 15 mins, (d) 30 mins, (e) 45 mins, (f) 1 hour.

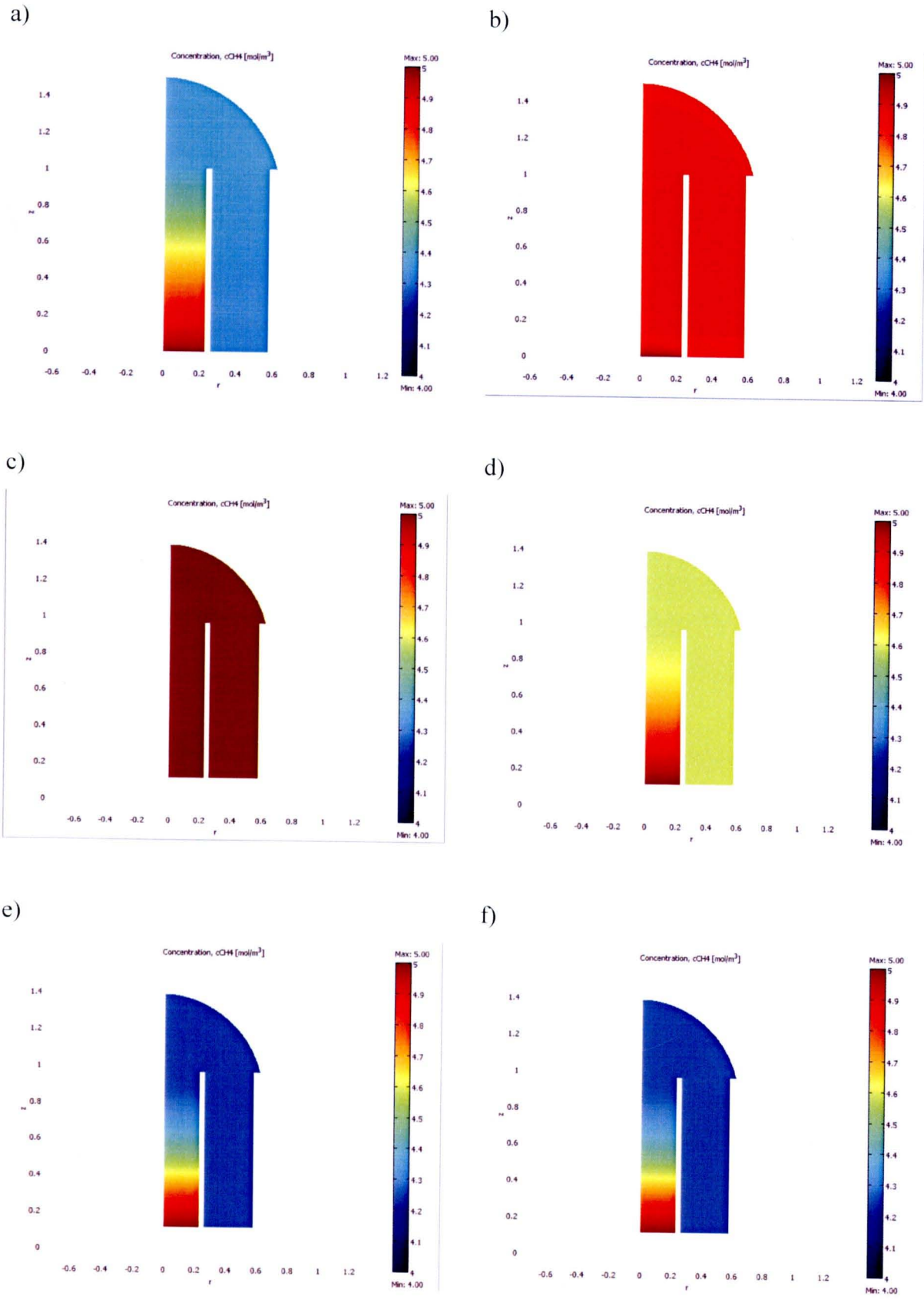


**Figure 4.11** Concentration of $CH_4$ along the cell for methane heat up gas at (a) 60s, (b) 6 mins, (c) 40 mins,(d) 1 hour, (e) 2 hours, (f) 4 hours.

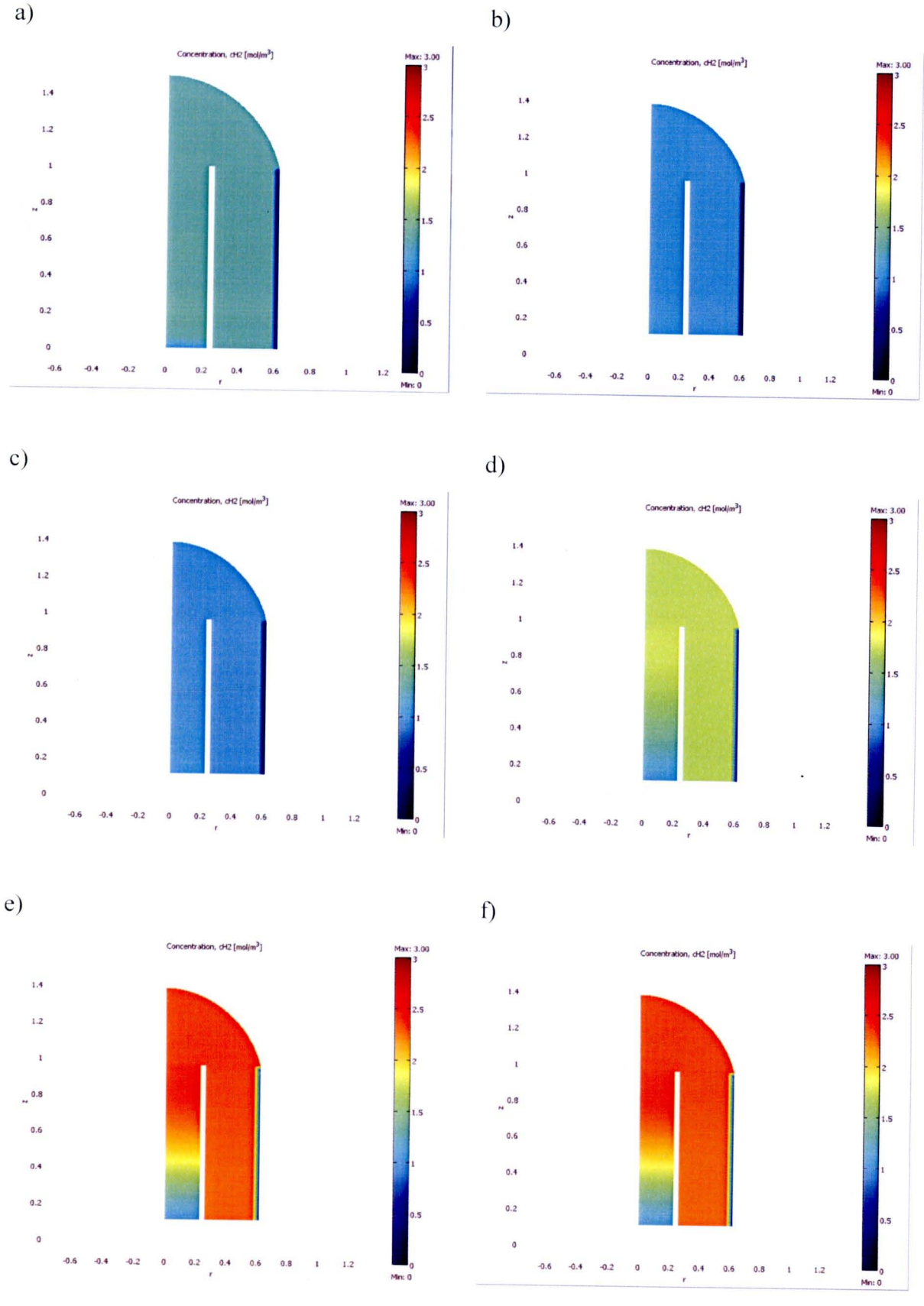


**Figure 4.12** Concentration of $H_2$ along the cell for methane heat up gas at (a) 60s, (b) 6 mins, (c) 40 mins,(d) 1 hour, (e) 2 hours, (f) 4 hours.

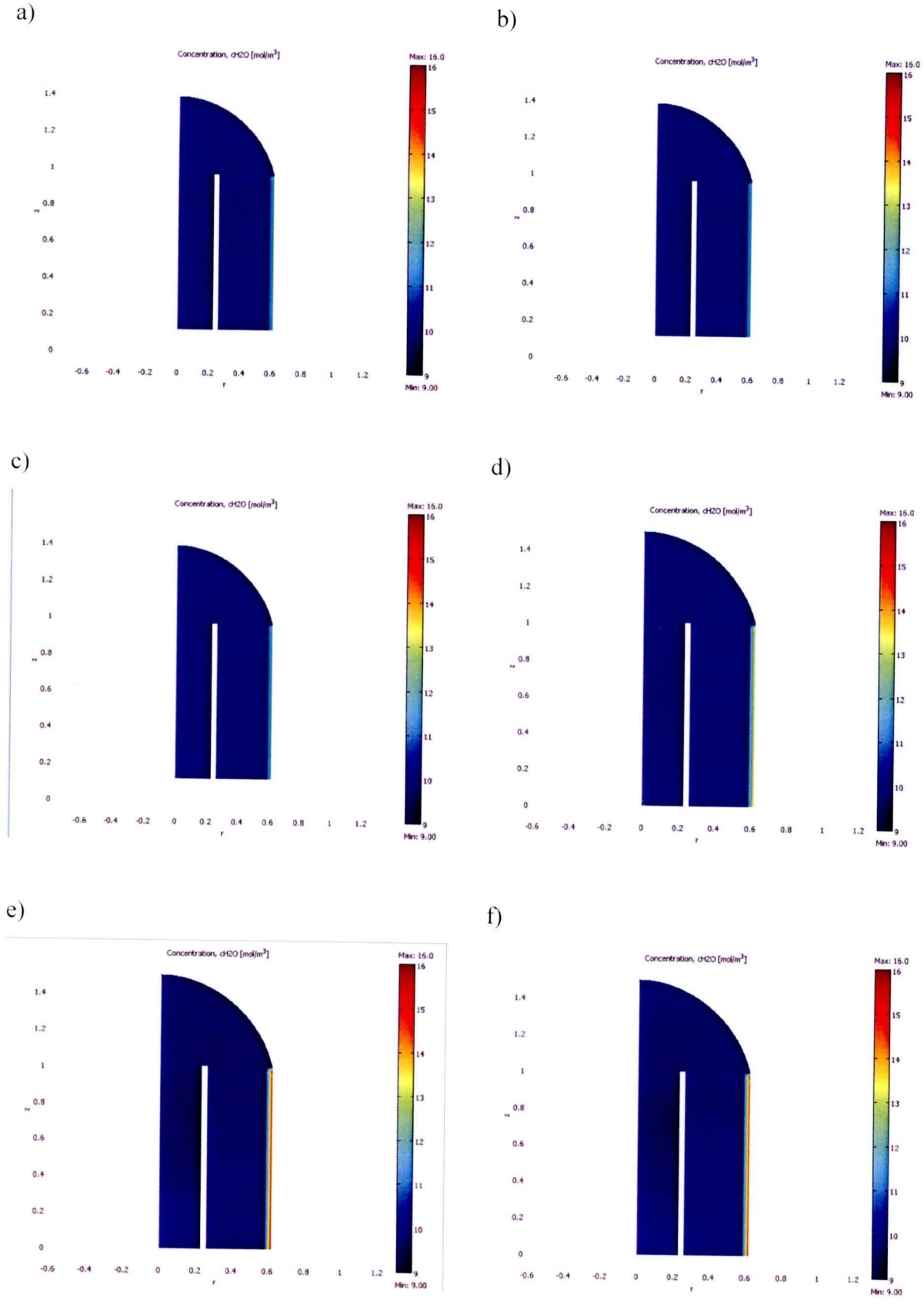


**Figure 4.13** Concentration of $H_2O$ along the cell for methane heat up gas at (a) 60s, (b) 6 mins, (c) 40 mins,(d) 1 hour, (e) 2 hours, (f) 4 hours.

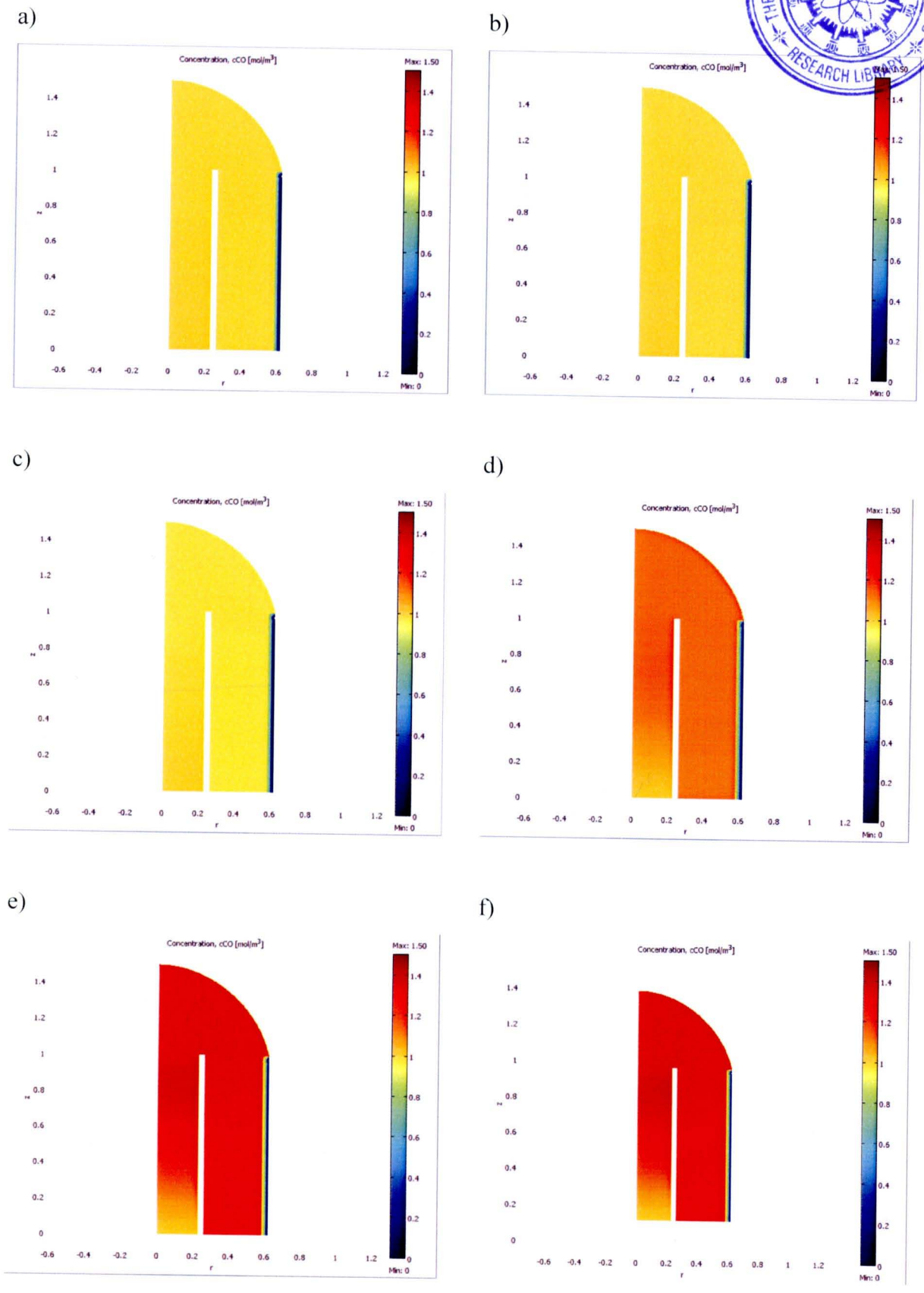


**Figure 4.14** Concentration of CO along the cell for methane heat up gas at (a) 60s, (b) 6 mins, (c) 40 mins,(d) 1 hour, (e) 2 hours, (f) 4 hours.

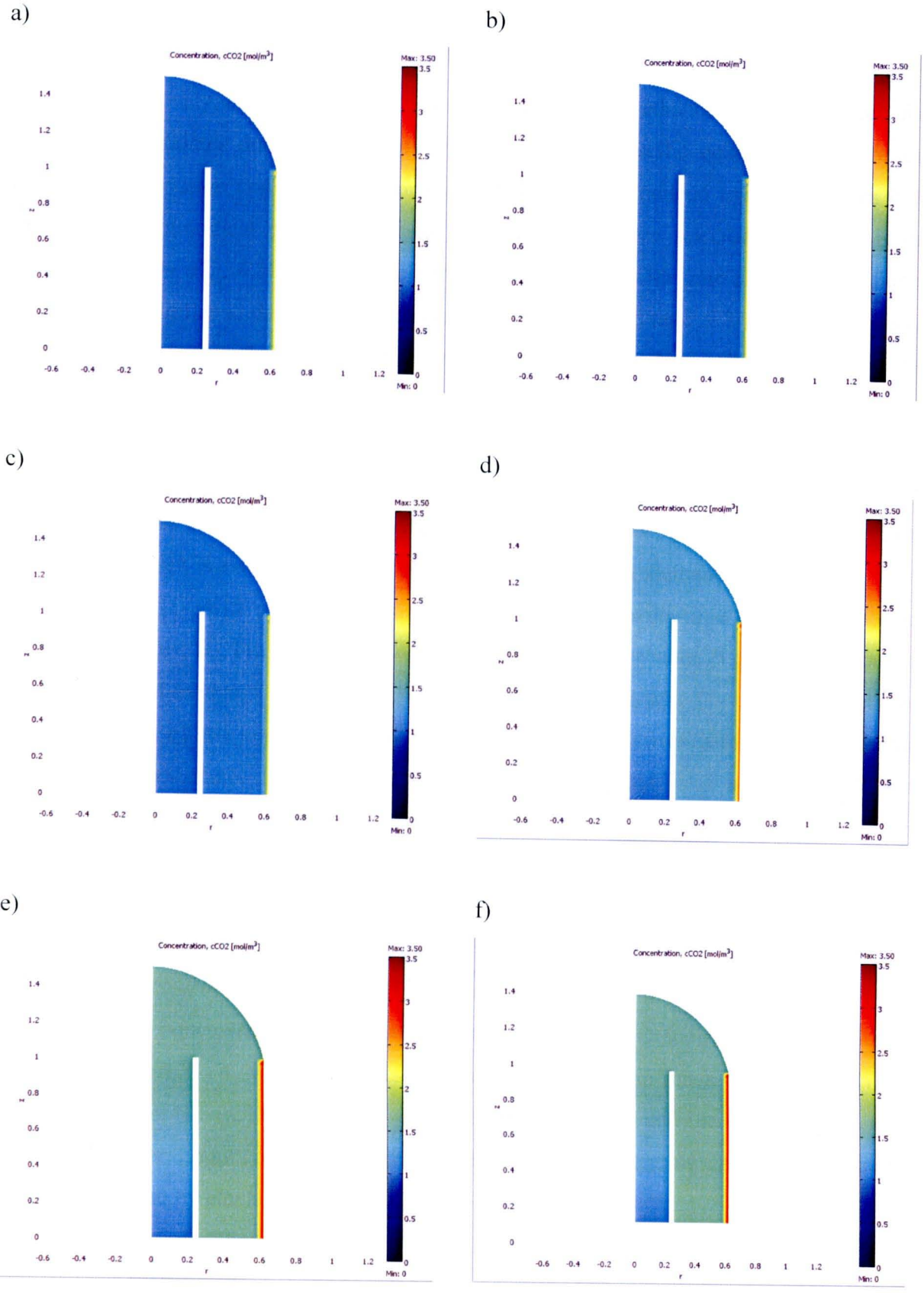


**Figure 4.15** Concentration of $CO_2$ along the cell for methane heat up gas at (a) 60s, (b) 6 mins, (c) 40 mins,(d) 1 hour, (e) 2 hours, (f) 4 hours.

### 4.1.5 IIR-SOFC heating up with alcohols (i.e. methanol and ethanol)

Alternatively, considering other potential primary fuels, ethanol and methanol are also interesting candidates due to their ready availability, high-specific energy, sulfur free and storage transportation convenience; moreover, they can be produced renewably from both chemical and biological processes. Hence these alcohols were selected for study as the heating-up gases. Fig. 4.10 presents the temperature gradient with time of IIR-SOFC fueled by methanol. Similar to the case of methane, the methanol (S/C ratio = 2/1) steam reforming reaction occurs first at the internal reformer prior to the electrochemical reaction at the fuel channel. It can be observed that the system temperature reaches 1173 K after 1.6 hours and reaches steady state after 5 hours. It should also be noted that the system temperature at the steady state condition for the case of IIR-SOFC fueled by methanol is less than that of hydrogen, syngas and methane. Furthermore, the heating-up rate for this case is observed to be 0.11 K/s, which is also less than that of hydrogen, syngas and methane.

Figs. 4.11- 4.15 present the concentration gradients with time for all compounds including $CH_3OH$, $H_2$, $H_2O$, CO and $CO_2$ along the IIR-SOFC system. It can be seen that the concentration of methanol decreases rapidly with the operating time (compared to methane) and the length of the system, which could be due to the lower reforming temperature requirement of methanol; hence methanol can be converted at the initial heating-up period to form $H_2$, CO and $CO_2$. Regarding the concentration profiles of $H_2$, $H_2O$, CO and $CO_2$, it was observed that the concentrations of $H_2$ and CO increase with increasing operating time, whereas those of $H_2O$ and $CO_2$ are rarely detect; this could possibly due to the low occurring of water-gas shift reaction due to the low S/C molar ratio applied.

For the case of IIR-SOFC fueled by ethanol (S/C ratio = 4/1), relatively similar trends of temperature concentration gradients with time as IIR-SOFC fueled by methanol were observed (Figs. 4.23- 4.28). Nevertheless, it takes shorter time to reach the SOFC operating temperature than IIR-SOFC fueled by methanol (around 7 min) and the temperature reaches steady state after 3 hours operation. It should be noted that the heating-up rate for the case of IIR-SOFC fueled by ethanol is observed to be 0.26 K/s.

a)

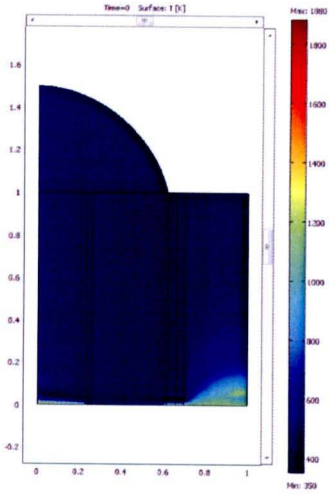

b)

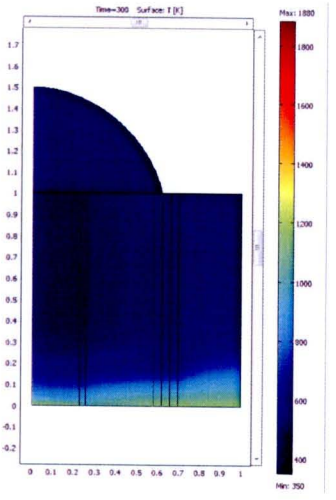

c)

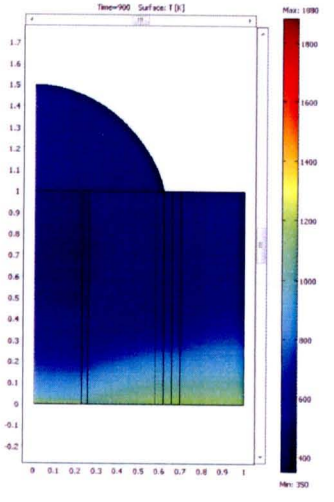

d)

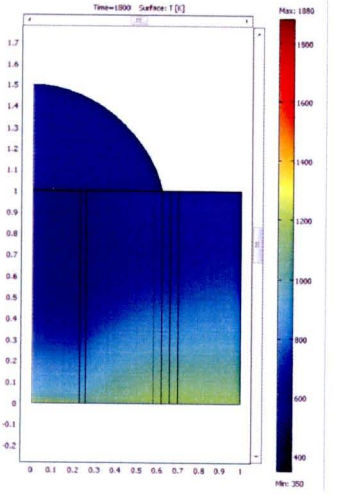

e)

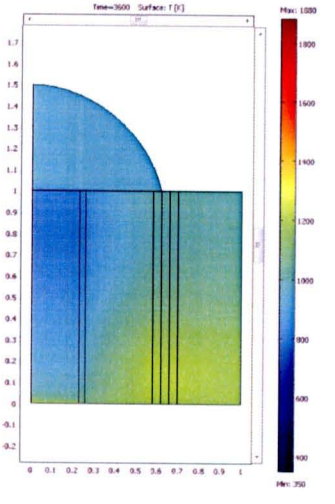

f)

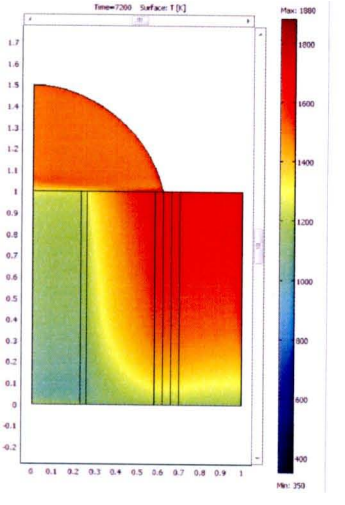

**Figure 4.16** Temperature distribution of heat-up by methanol at (a) 0s, (b) 5 mins, (c) 15 mins,(d) 30 mins, (e) 1 hour, (f) 2 hours.

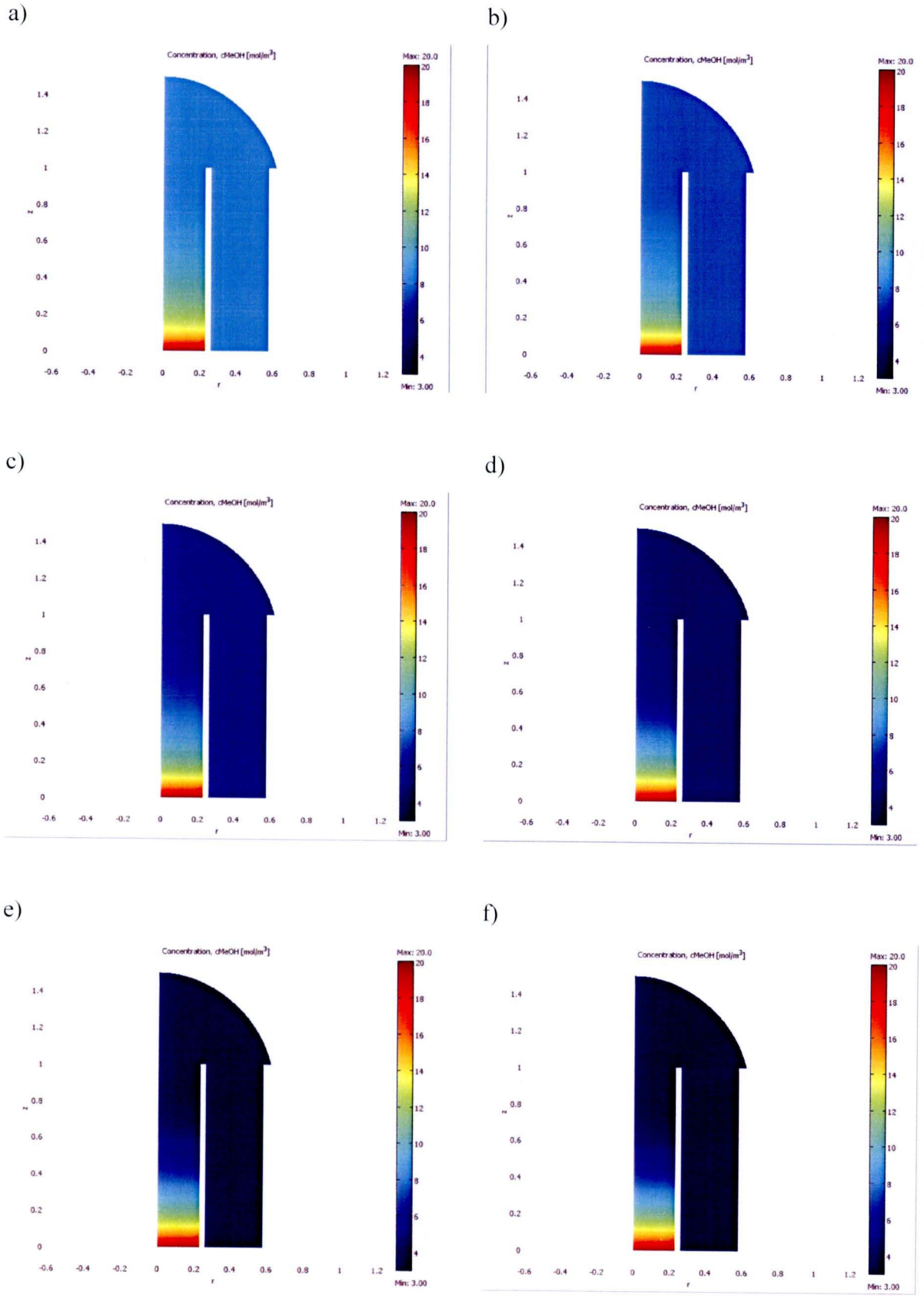


**Figure 4.17** Concentration of $CH_3OH$ along the cell for methanol heat up gas at at (a) 60s, (b) 6 mins, (c) 24 mins,(d) 1 hour, (e) 2 hours, (f) 5 hours.

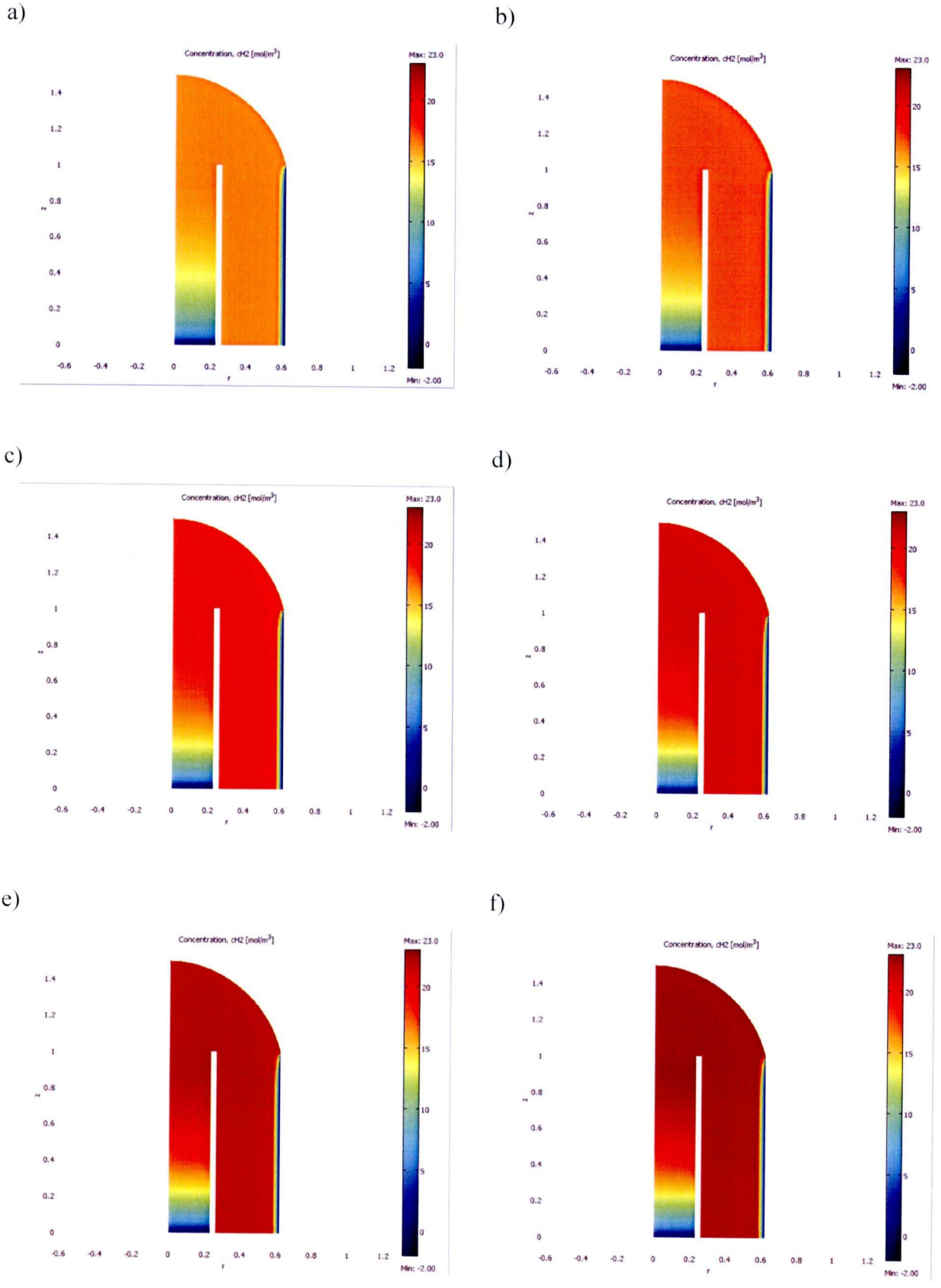


**Figure 4.18** Concentration of $H_2$ along the cell for methanol heat up gas at at (a) 60s, (b) 6 mins, (c) 24 mins,(d) 1 hour, (e) 2 hours, (f) 5 hours.

a)

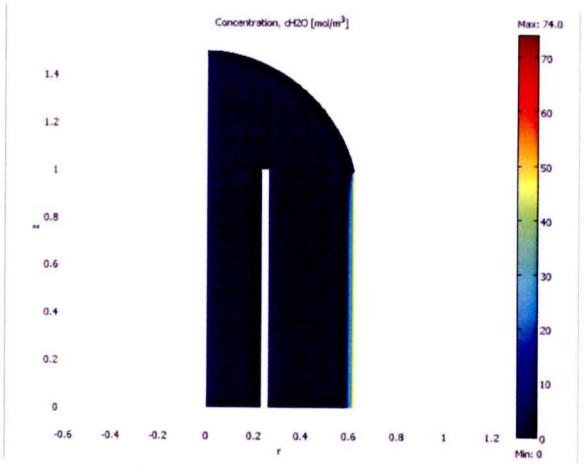


b)

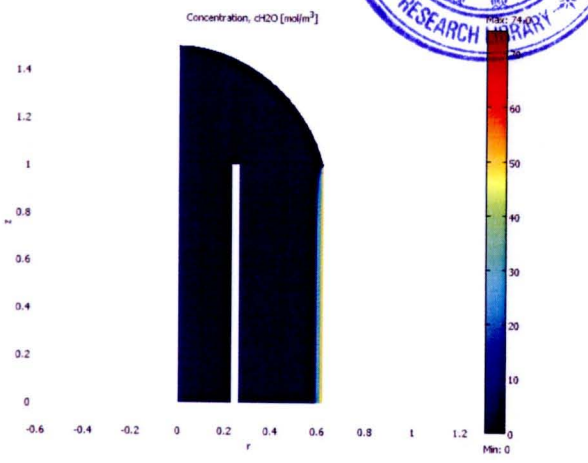


c)

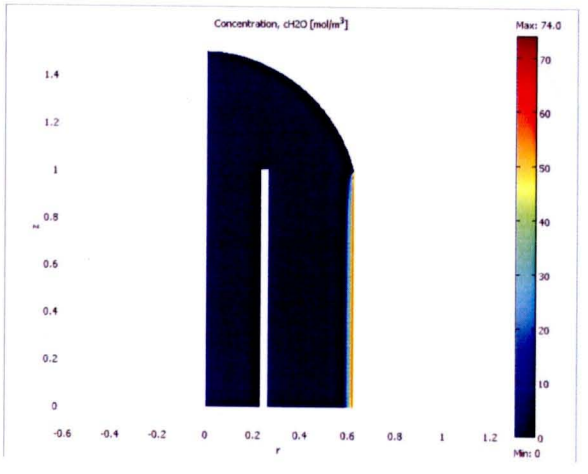


d)

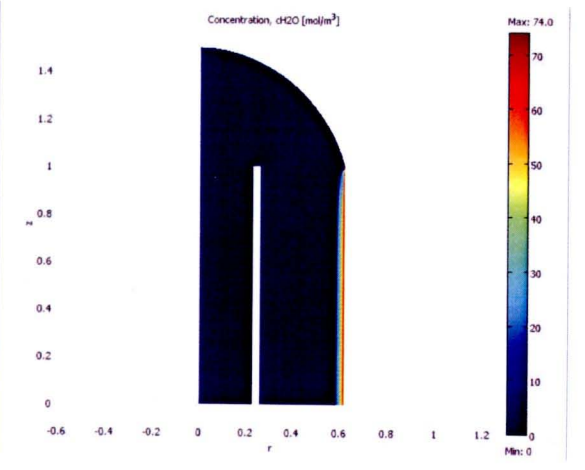


e)

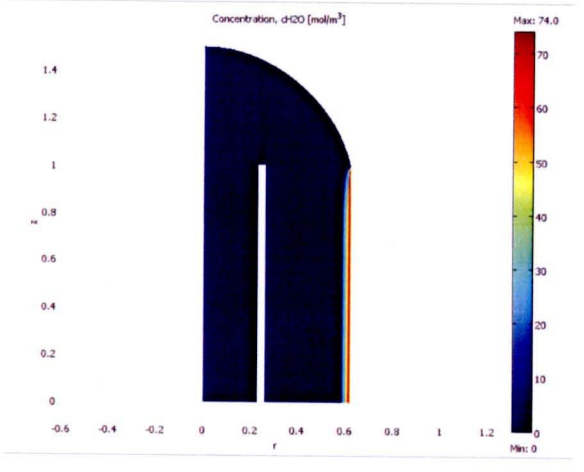


f)

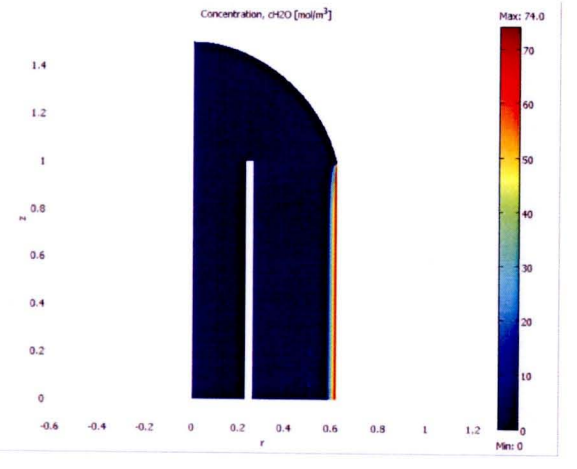


**Figure 4.19** Concentration of $H_2O$ along the cell for methanol heat up gas at at (a) 60s, (b) 6 mins, (c) 24 mins,(d) 1 hour, (e) 2 hours, (f) 5 hours.

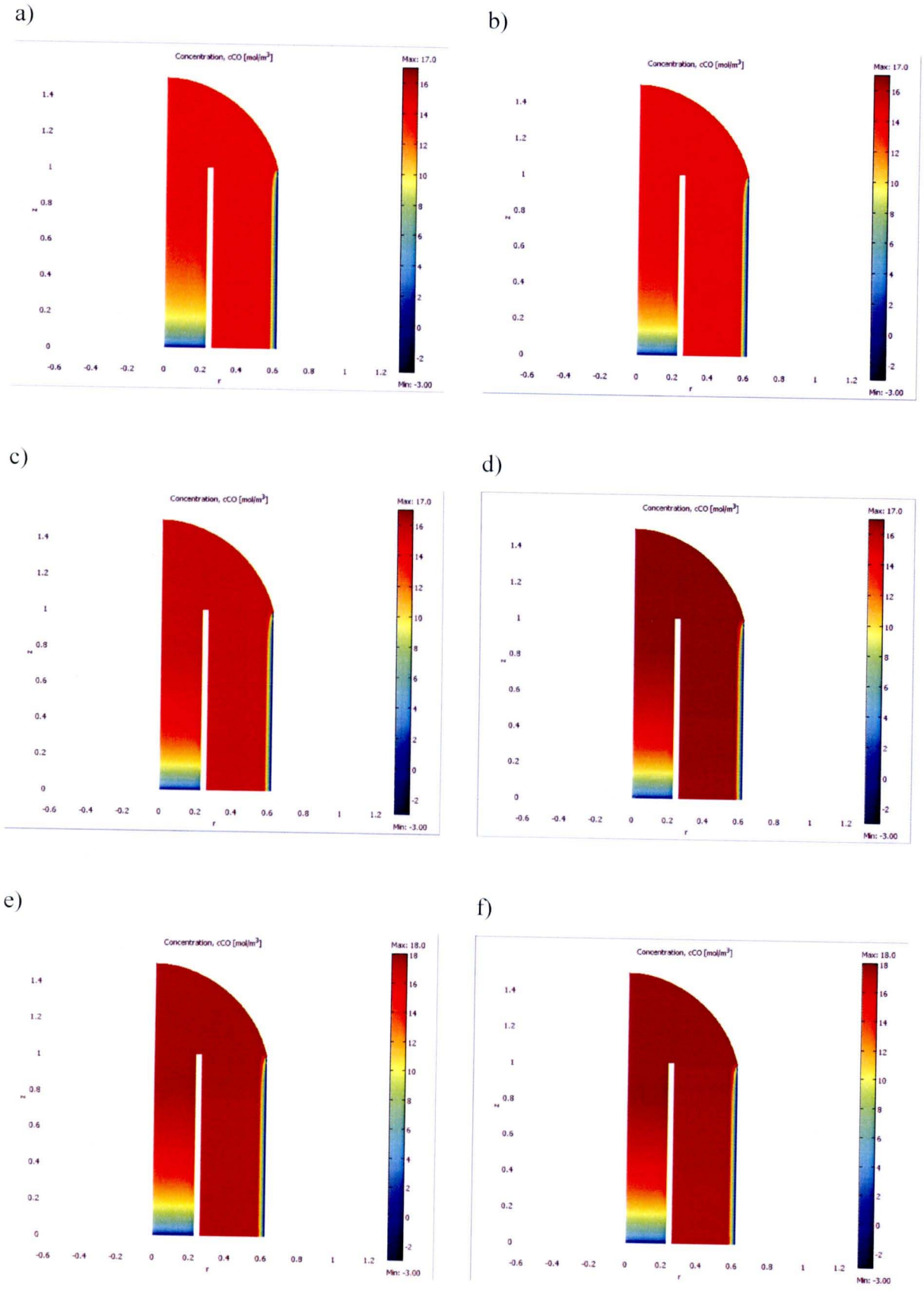


**Figure 4.20** Concentration of CO along the cell for methanol heat up gas at at (a) 60s, (b) 6 mins, (c) 24 mins,(d) 1 hour, (e) 2 hours, (f) 5 hours.

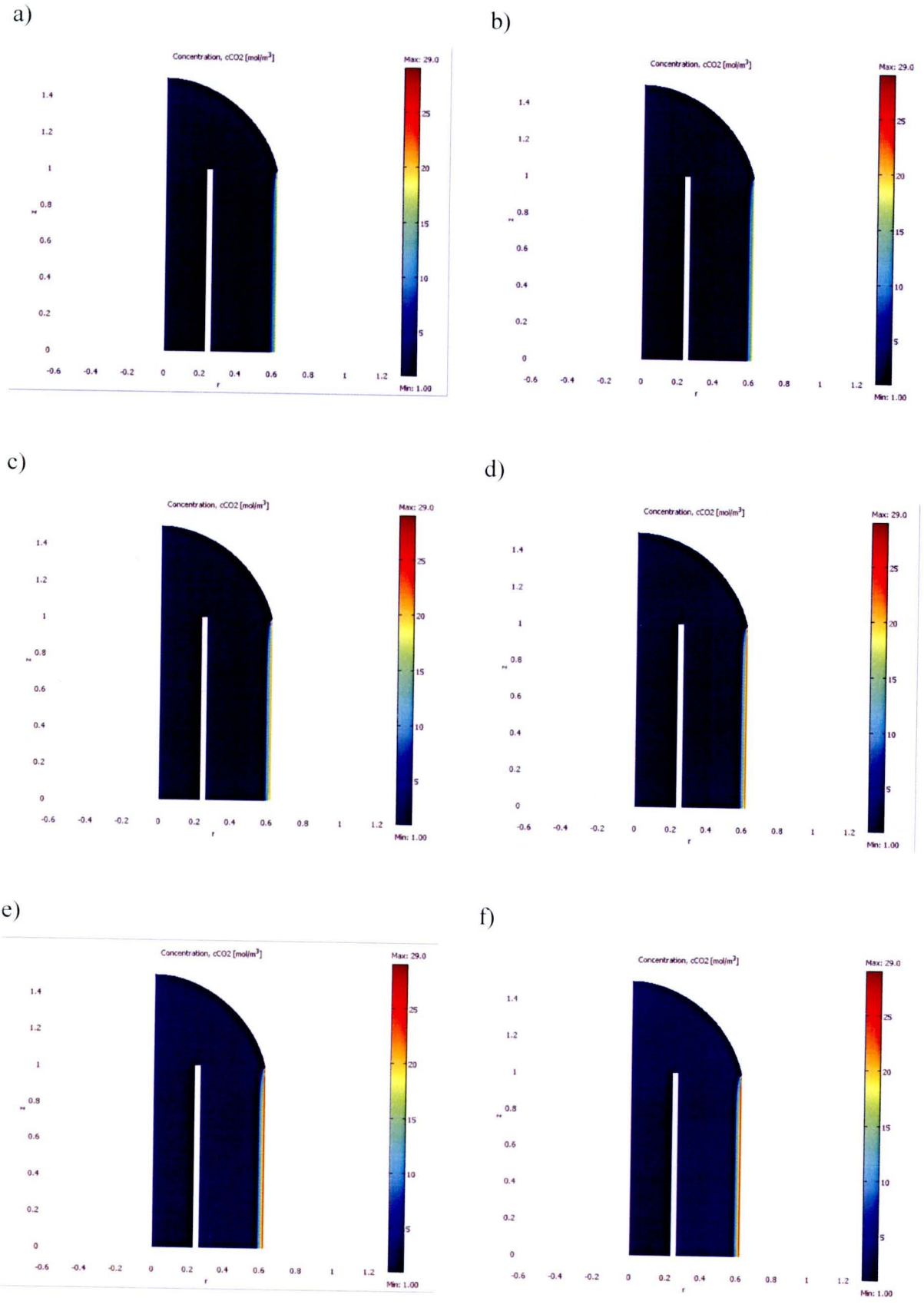


**Figure 4.21** Concentration of $CO_2$ along the cell for methanol heat up gas at at (a) 60s, (b) 6 mins, (c) 24 mins,(d) 1 hour, (e) 2 hours, (f) 5 hours

a)

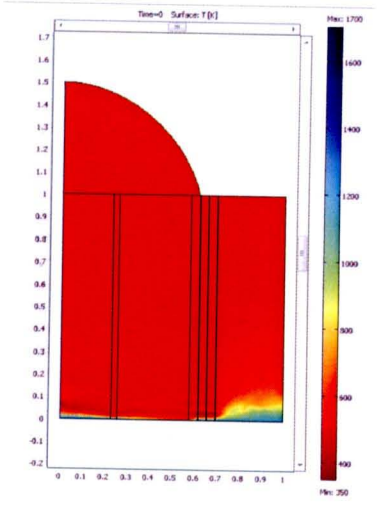

b)

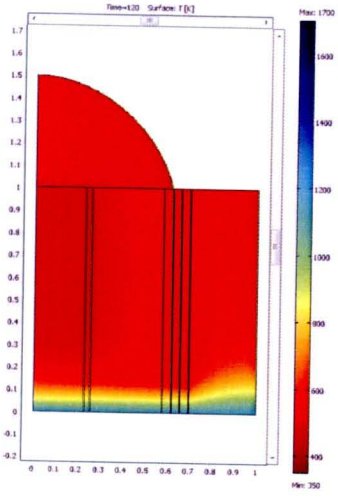

c)

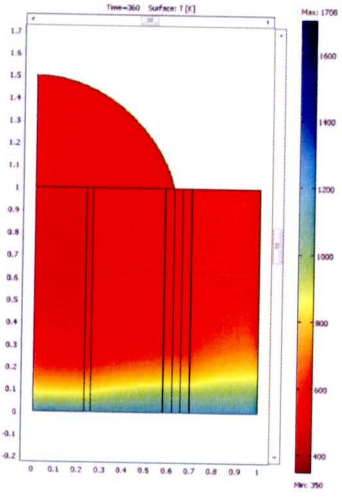

d)

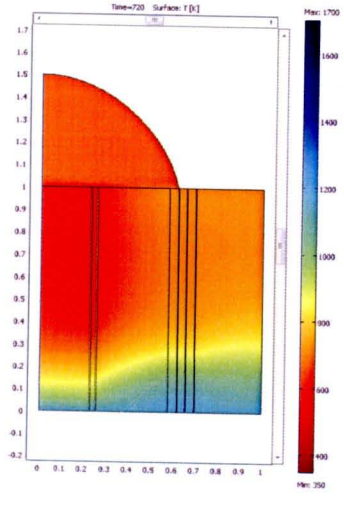

e)

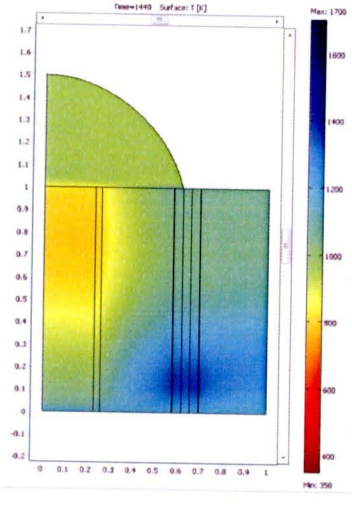

f)

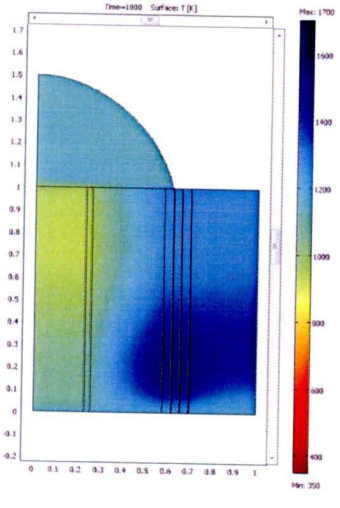

**Figure 4.22** Temperature distribution of heat-up by ethanol at (a) 0s, (b) 2 mins, (c) 6 mins,(d) 12 mins, (e) 45 mins, (f) 1 hour

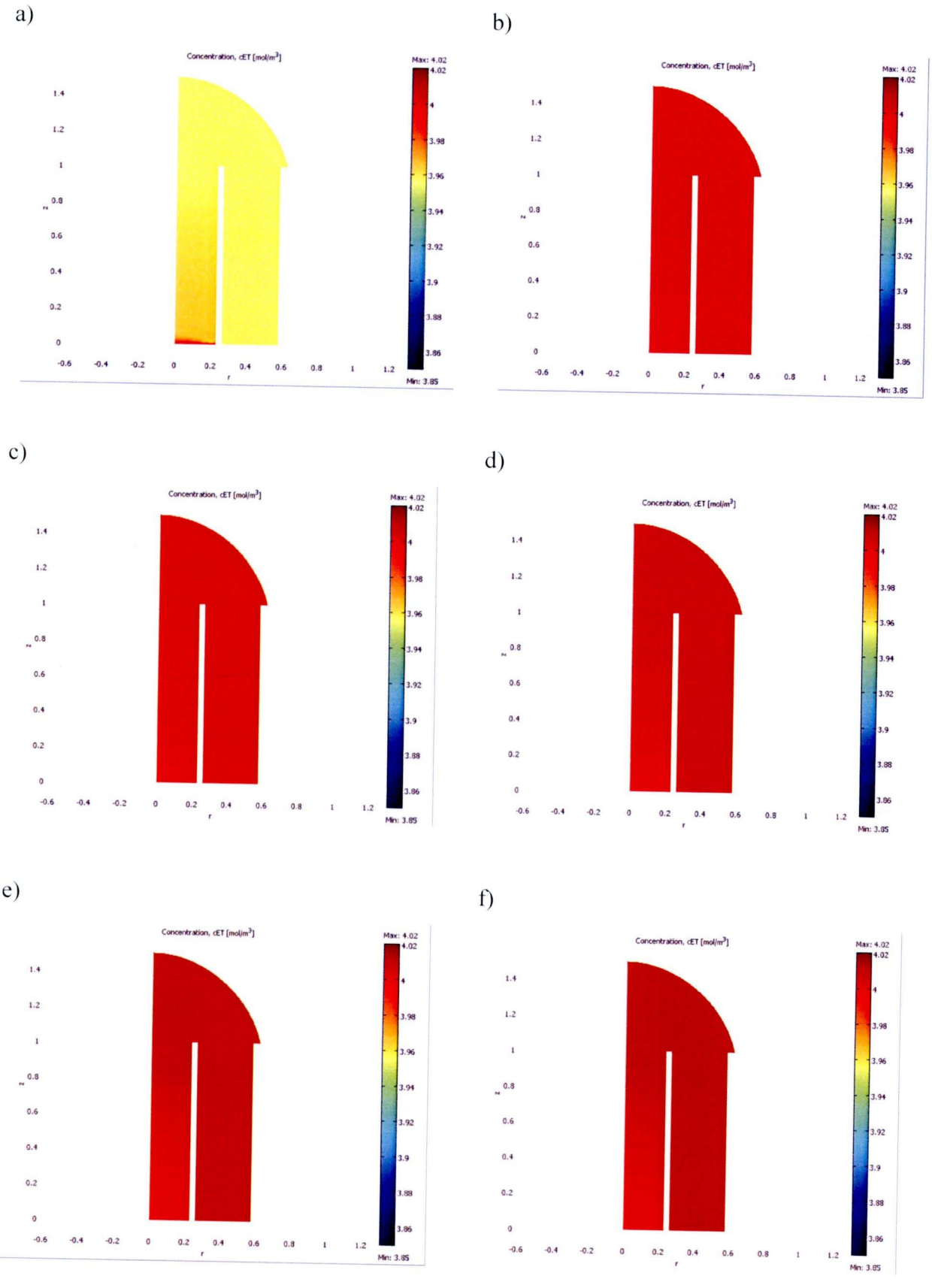


**Figure 4.23** Concentration of $C_2H_5OH$ along the cell for ethanol heat up gas at (a) 60s, (b) 6 mins, (c) 30mins,(d) 1 hour, (e) 2 hours, (f) 4 hours

a)

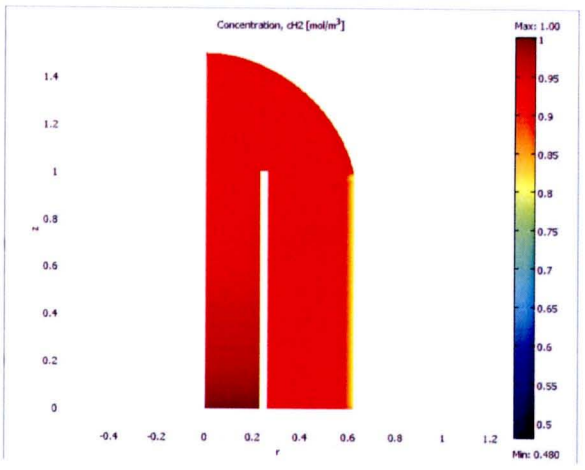


b)

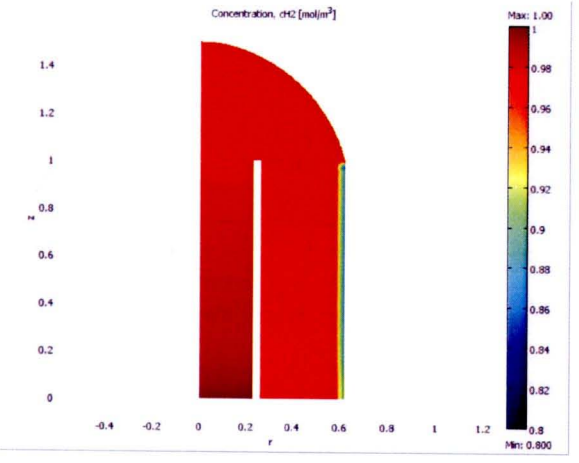


c)

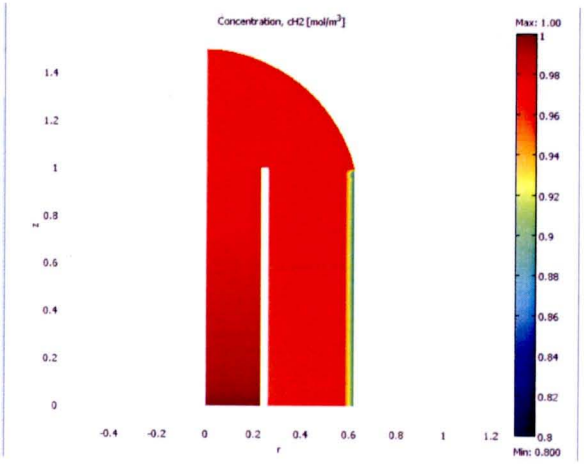


d)

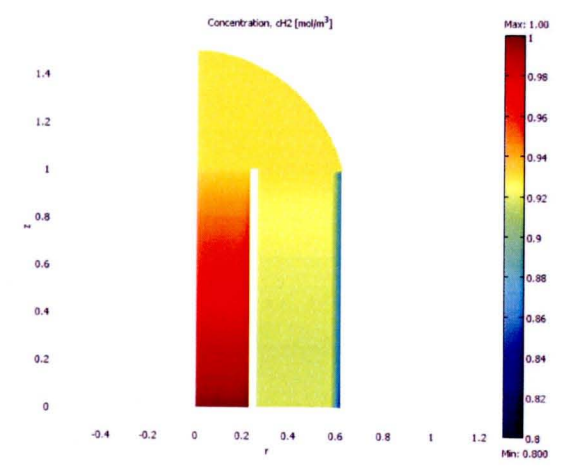


e)

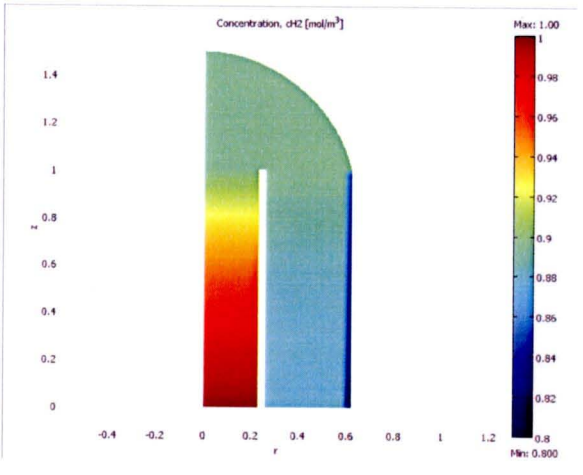


f)

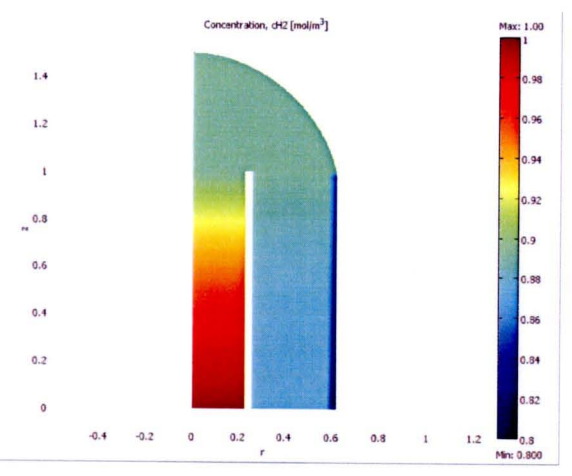


**Figure 4.24** Concentration of $H_2$ along the cell for ethanol heat up gas at (a) 60s, (b) 6 mins, (c) 30mins,(d) 1 hour, (e) 2 hours, (f) 4 hours

a)

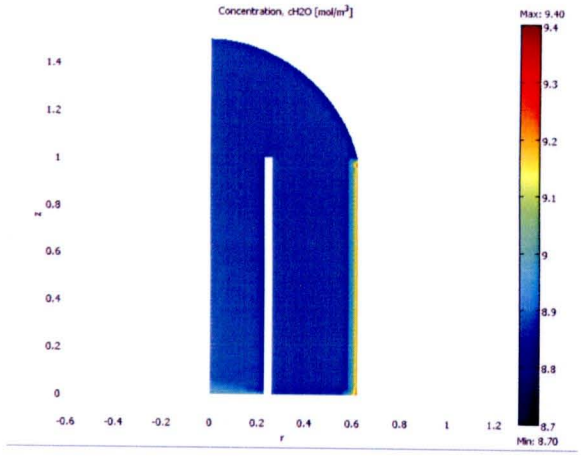


b)

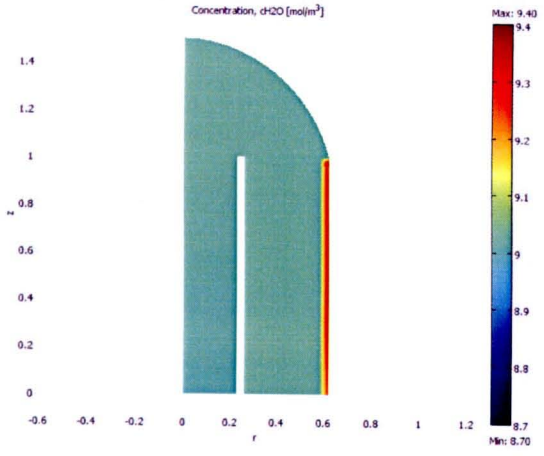


c)

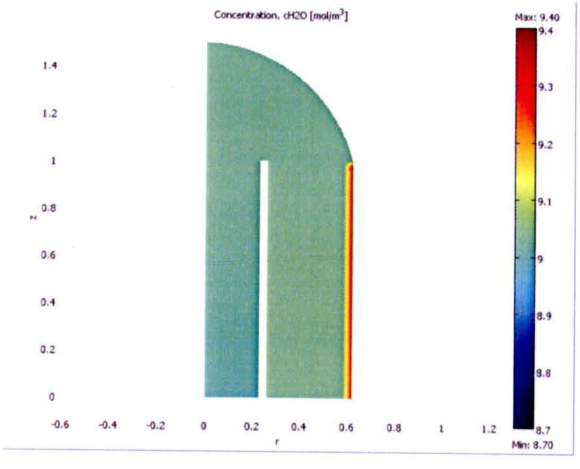


d)

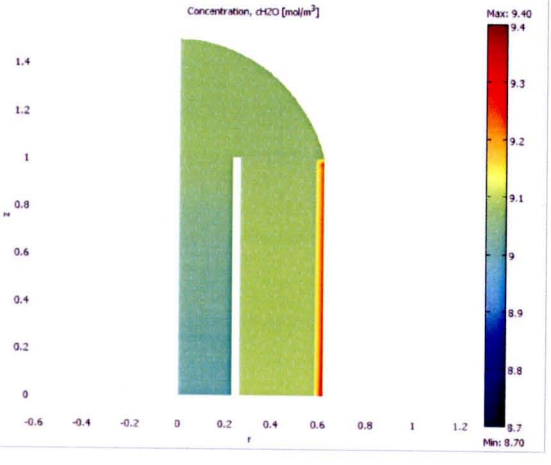


e)

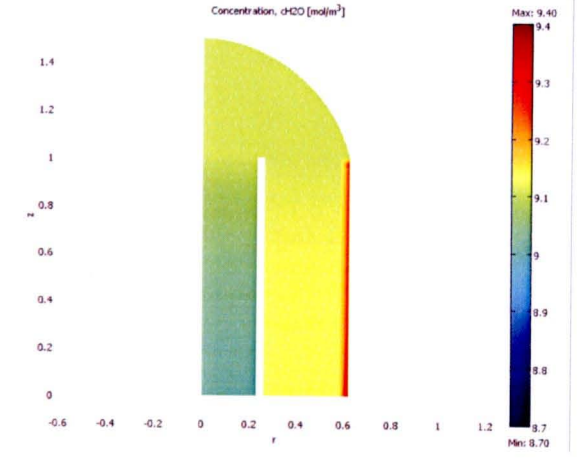


f)

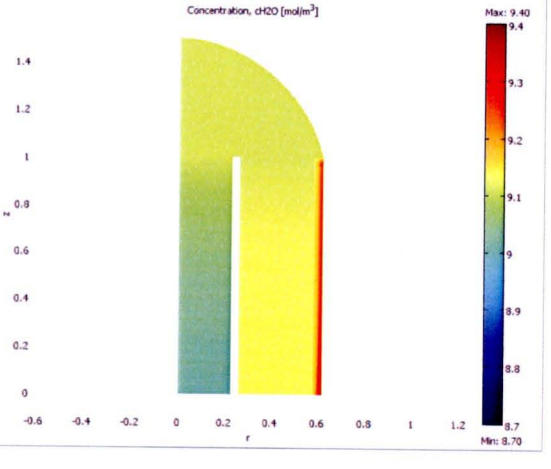


**Figure 4.25** Concentration of $H_2O$ along the cell for ethanol heat up gas at (a) 60s, (b) 6 mins, (c) 30mins,(d) 1 hour, (e) 2 hours, (f) 4 hours

a)

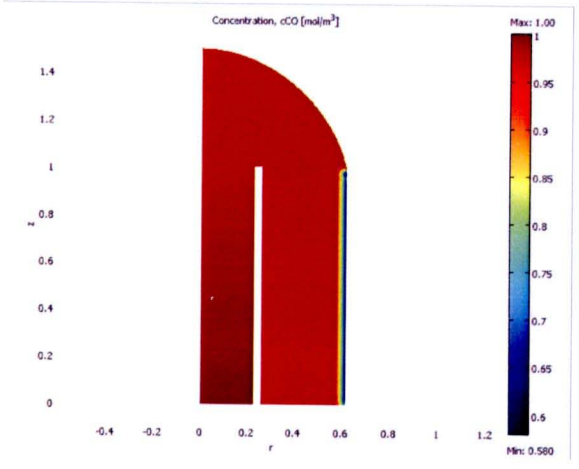


b)

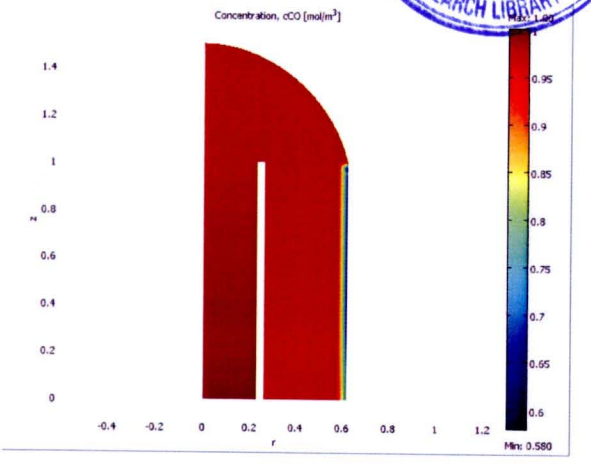


c)

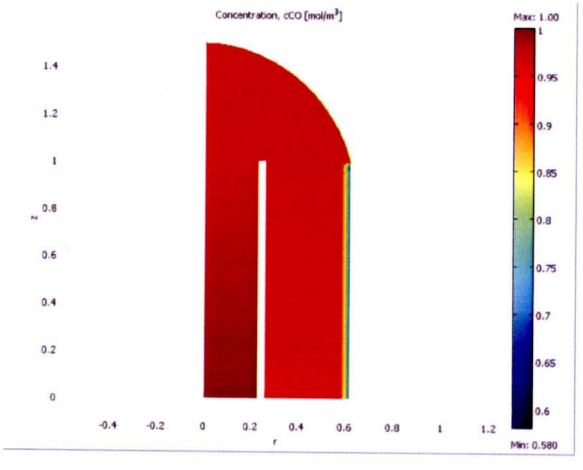


d)

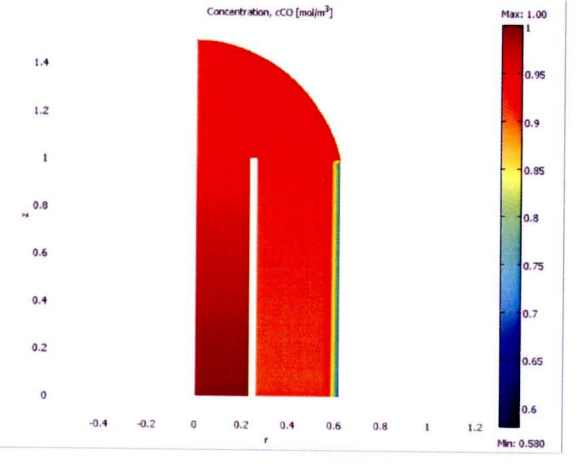


e)

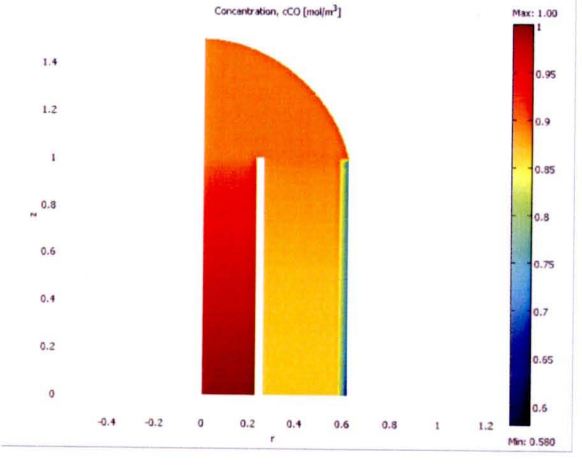


f)

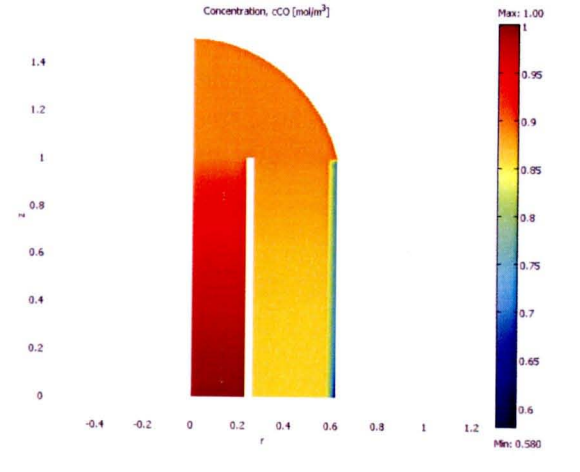


**Figure 4.26** Concentration of CO along the cell for ethanol heat up gas at (a) 60s, (b) 6 mins, (c) 30mins,(d) 1 hour, (e) 2 hours, (f) 4 hours

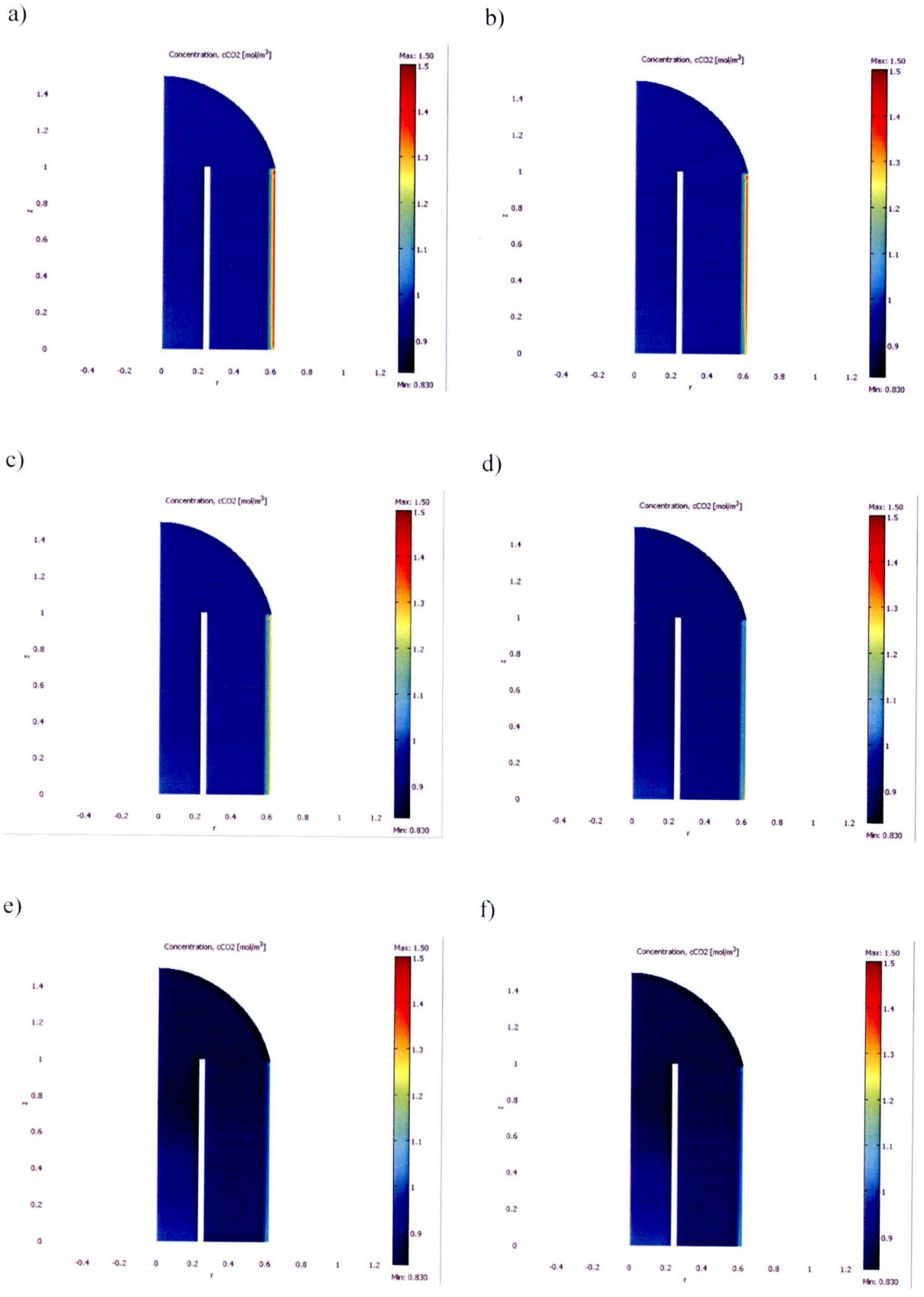


**Figure 4.27** Concentration of $CO_2$ along the cell for ethanol heat up gas at (a) 60s, (b) 6 mins, (c) 30mins,(d) 1 hour, (e) 2 hours, (f) 4 hours

For a clear comparison, Fig. 4.29 summarised the temperature rising with time during starting-up period for SOFC fueled by various gases. As explained earlier, except for the heating up with nitrogen, the temperature at the steady state in the case of SOFC fueled by methanol is the lowest. Fig. 4.30 compares the temperature profile at the initial heating-up (1 hour). It is clear that the temperature gradient with time for the case12 of methanol is the smoothest (from the calculation the heating rate for the cases of SOFC heated by nitrogen, hydrogen, syngas, methane, methanol and ethanol are 0.006 K/s, 0.93 K/s, 0.37 K/s, 0.31 K/s, 0.11 K/s and 0.26 K/s respectively.

It is noted that the profile of power density with time from this SOFC system was also predicted. As shown in Fig. 4.31, the power densities from SOFC fueled by hydrogen and syngas are relatively higher than those from IIR-SOFC fueled by hydrocarbon fuels. Among the hydrocarbon fuels, SOFC fueled by methanol seems to obtain the highest power density at a steady state condition.

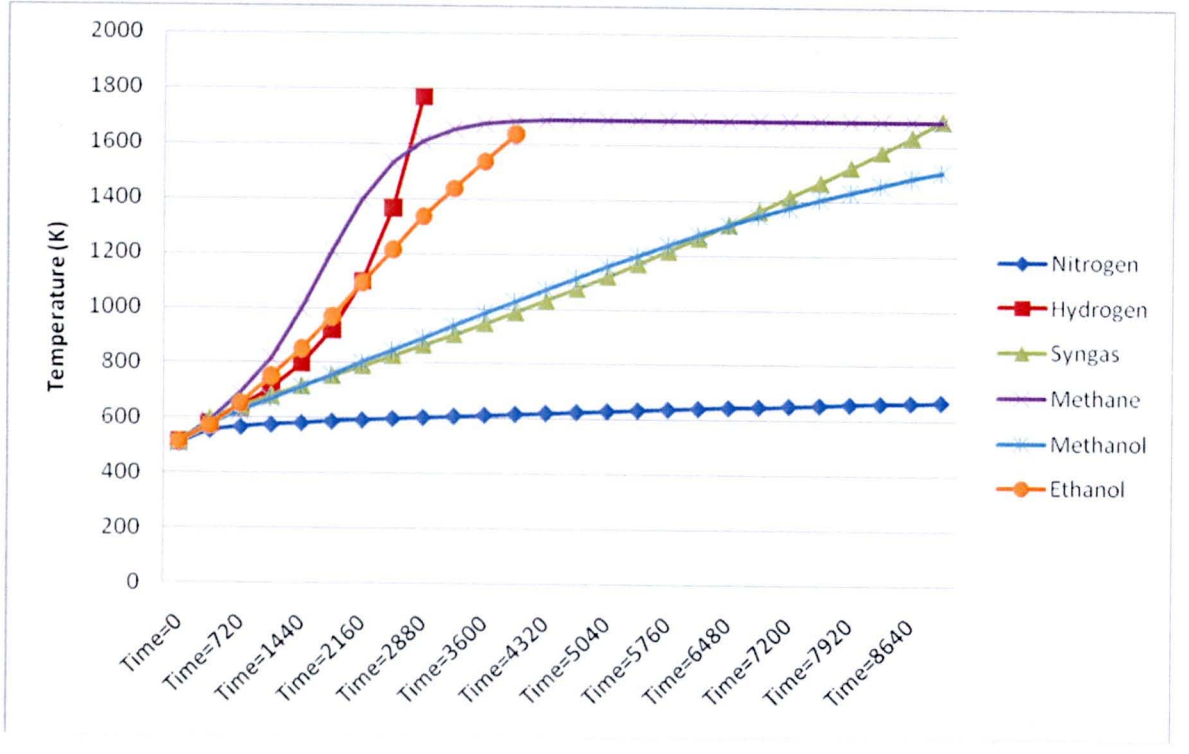


**Figure 4.28** Temperature profile by time fueled by heat up gases during start up period

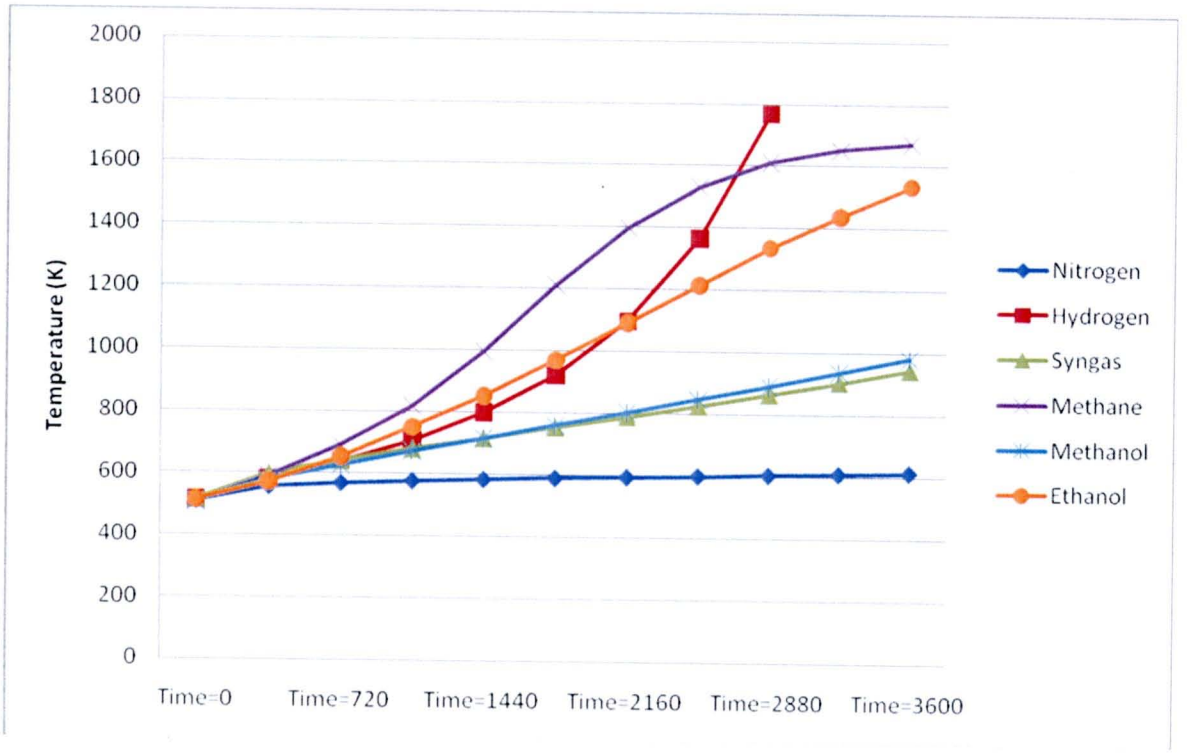


**Figure 4.29** Temperature profile by time each heat up gases in first hours

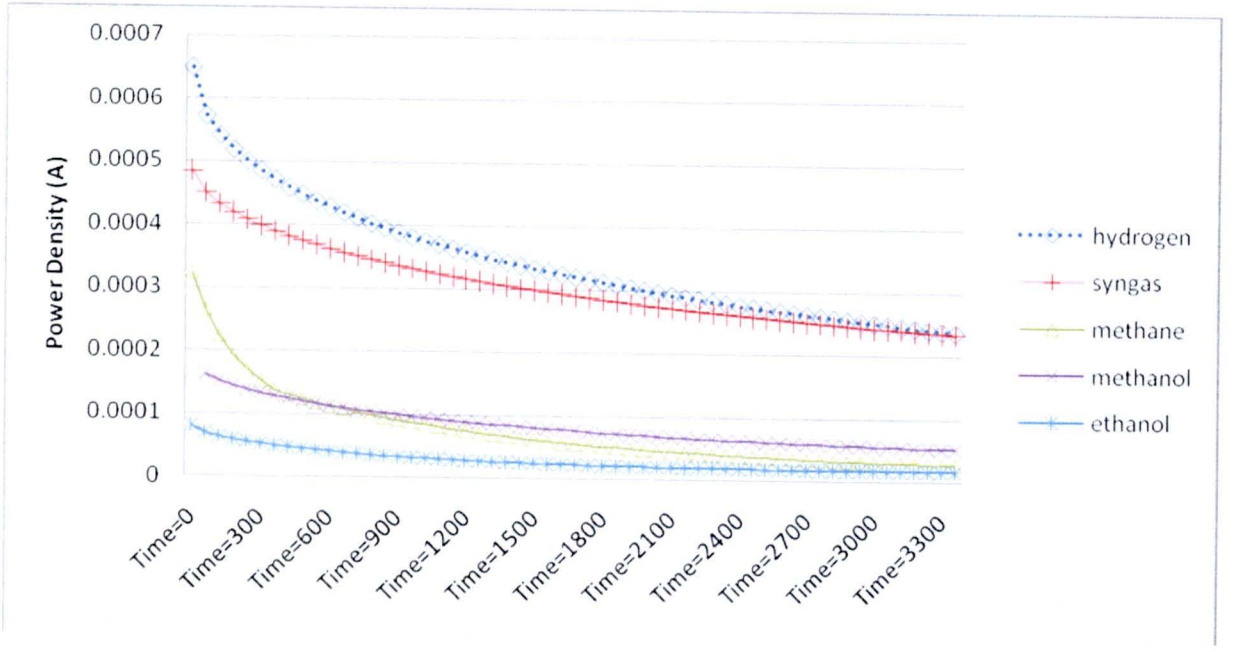


**Figure 4.30** Power density profile by time each heat up gases in first hour

### 4.2.6 Effect of inlet S/C ratio

Lastly, as the thermodynamic properties of inlet fuels are important factors for the thermal behavior of SOFC system, the effect of inlet steam/carbon (S/C) ratio for IIR-SOFC fueled by hydrocarbon fuels (i.e. methane, methanol and ethanol) was studied and compared by varying the S/C ratio from 2.0 to 3.0 and 4.0. As shown in Figs. 4.32- 4.34, it was found that the changing of inlet S/C ratio does not show much effect on the heating rate during starting-up period for all types of hydrocarbon feeds. Nevertheless, it noticeably affects the temperature of the system at steady state condition, from which the use of high S/C molar ratios (S/C ratio of 4.0) results in the higher system temperature. Therefore, this leads to the lower power density achievement at steady state condition (as presented in Figure. 4.35).

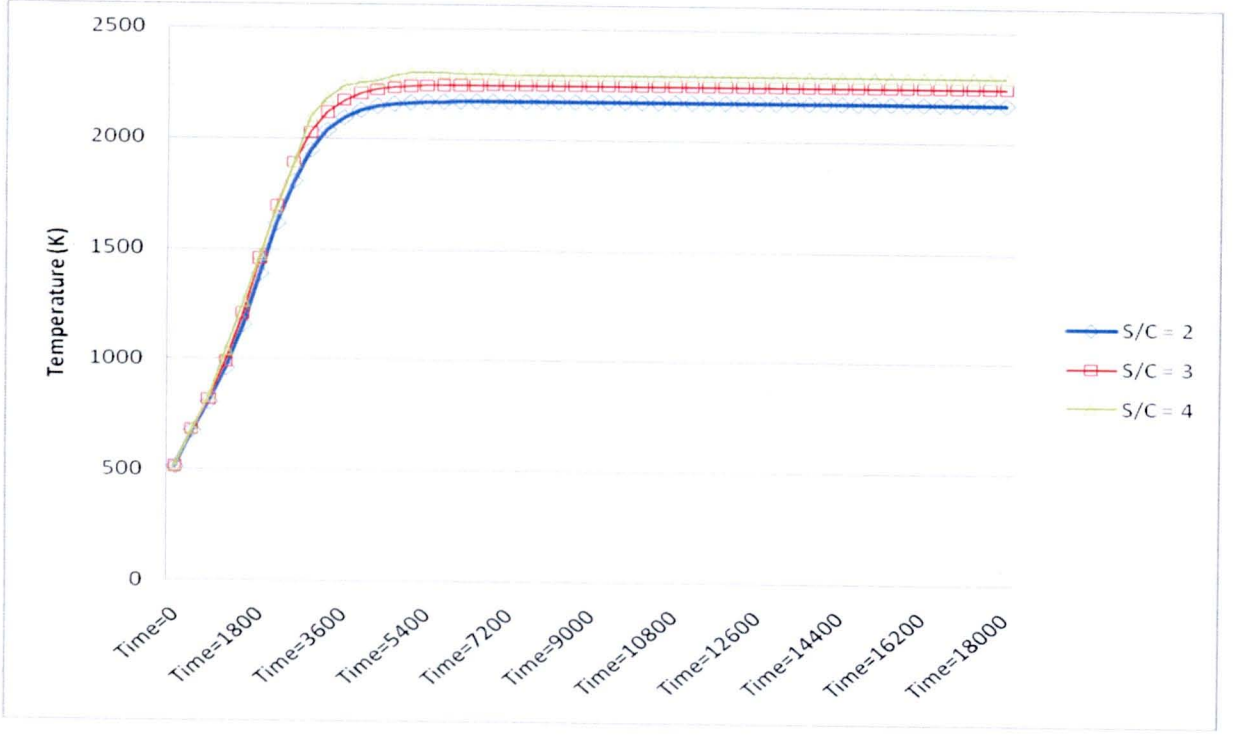


**Figure 4.31** The effect on temperature profile of S/C ratio of IIR-SOFC fueled by methane

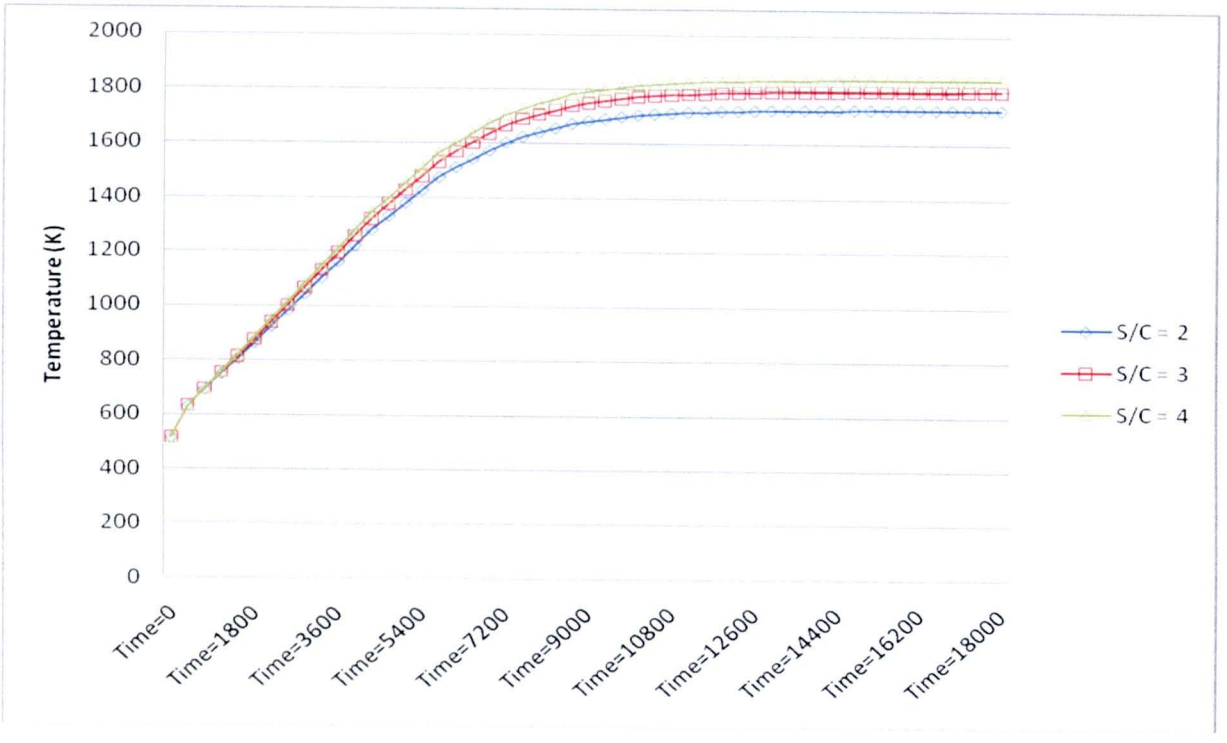


**Figure 4.32** The effect on temperature profile of S/C ratio of IIR-SOFC fueled by methanol

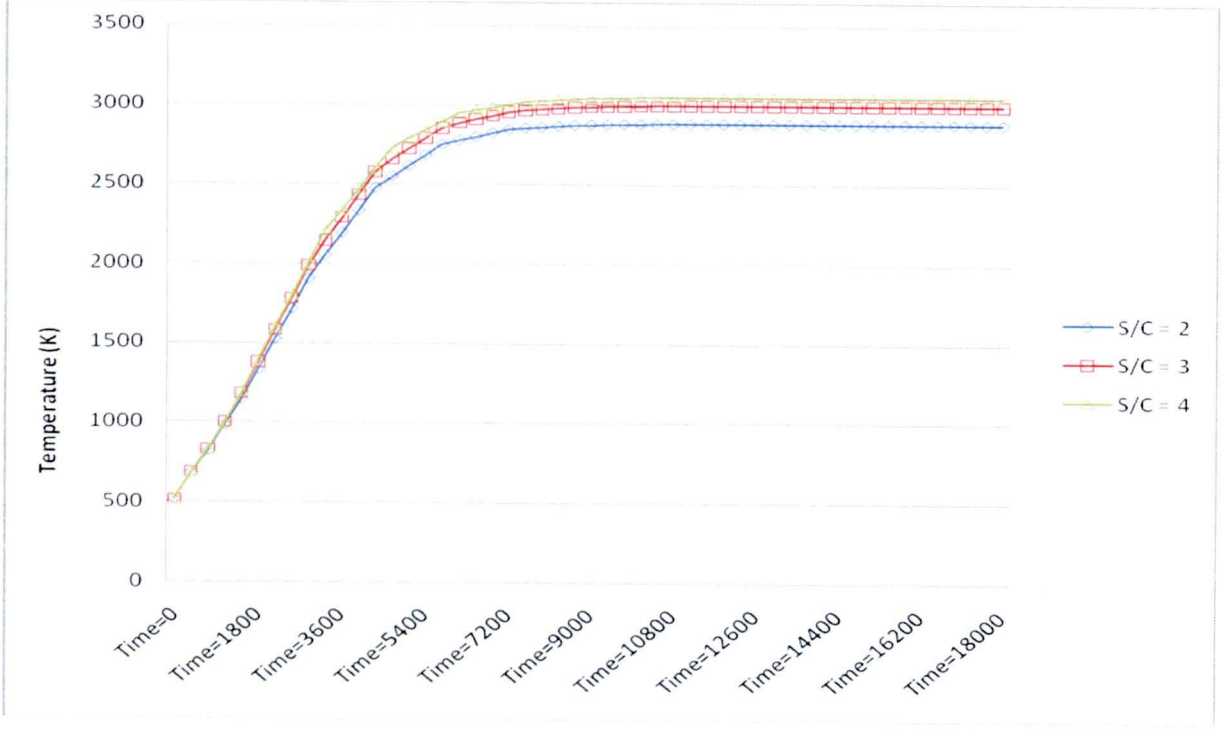


**Figure 4.33** The effect on temperature profile of S/C ratio of IIR-SOFC fueled by ethanol

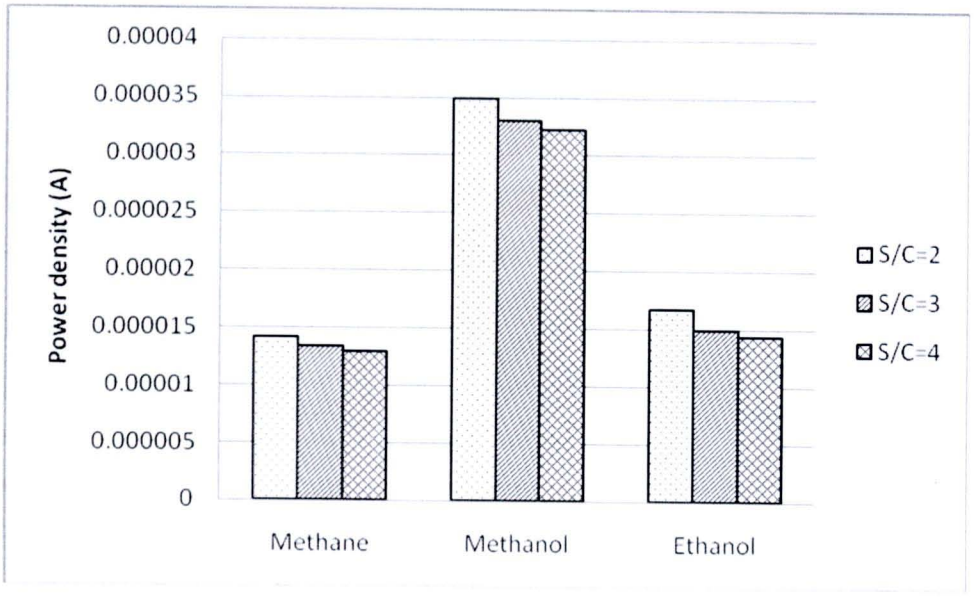


**Figure 4.34** The effect on power density of S/C ratio of IIR-SOFC

### 4.2.7 Effect of inlet flow direction

Theoretically, as for a typical heat exchanging system, flow direction of heat exchanged fluids strongly affects the heat transfer and reaction behavior in the fluid steam, thus the effect of fuel and oxidant flow direction on the IIR-SOFC performance was also considered. In the previous section, air flow is counter flow to fuel flow in SOFC fuel channel (a so-called 'counter-flow' pattern). As an alternative, fuel and air steam can be passed in the same direction, a so-called as 'co-flow' pattern. The system behavior of co-flow pattern was analyzed by changing mass and energy balances in air channel along with their corresponding boundary conditions while keeping all other operating conditions identical to those of counter-flow pattern. Figure 4.35 shows the temperature profile along all channels of an IIR-SOFC with co-flow pattern compared with the data in figure 4.28. It can be seen that the flow direction of co-flow pattern is smoother than counter flow pattern. IIR-SOFC with co-flow pattern is due to the good matching between the heat exothermically supplied from electrochemical reaction and heat required for endothermic steam reforming along the SOFC system. Thus it is concluded that an IIR-SOFC with co-flow pattern is more satisfactory than that with counter-flow pattern.

In terms of power density, co-flow pattern leads to the higher power density achievement at steady state condition.

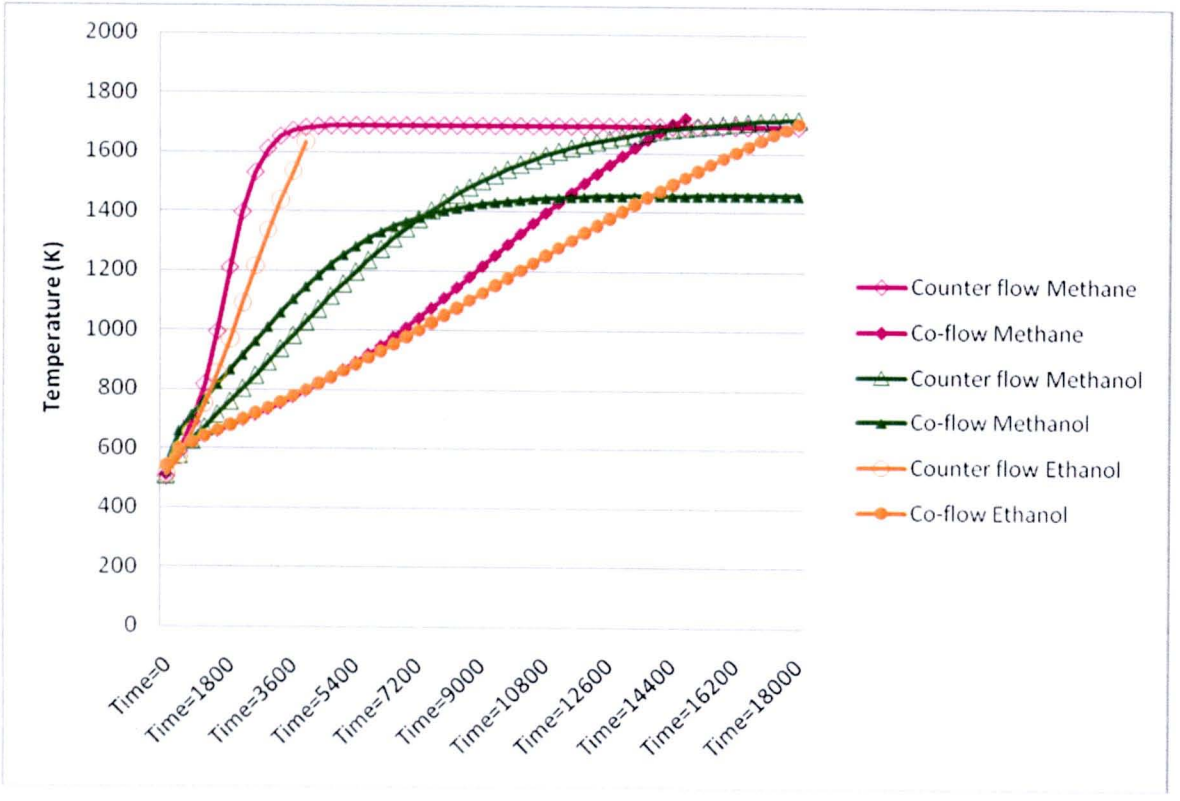


**Figure 4.35** Temperature profile by time fueled by heat up gases during start up perioed with inlet flow pattern.

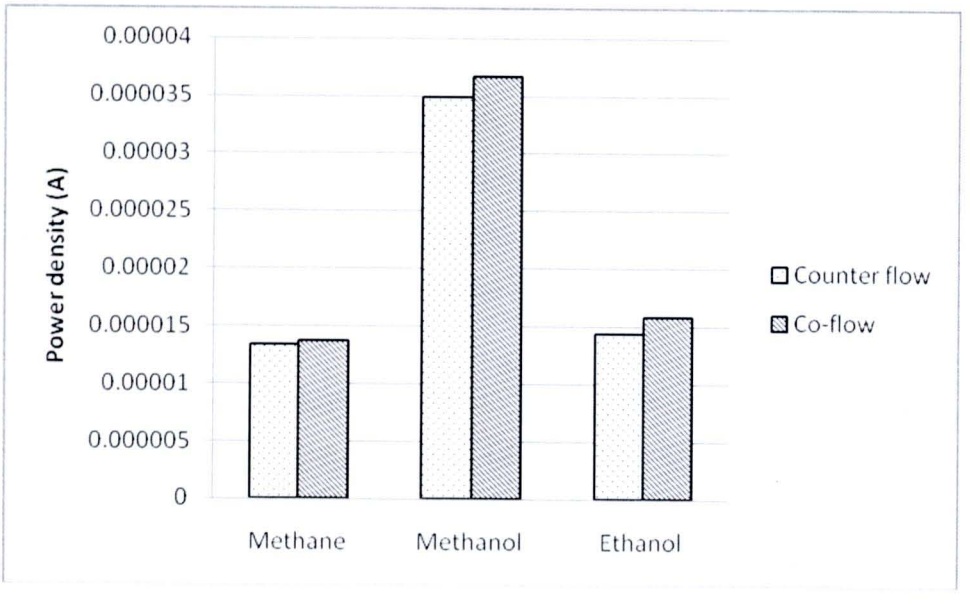


**Figure 4.36** The effect on power density of inlet flow pattern